暗物质的引力波和射电信号探测

黄发朋 (Fa Peng Huang)
中山大学物理与天文学院&天琴中心

FPH, K. Kadota, T. Sekiguchi, H. Tashiro, Phys.Rev. D97 (2018) no.12, 123001
James Buckley, Bhupal Dev, Francesc Ferrer, FPH, *Phys.Rev.D* 103 (2021) 4, 043015
Haipeng An, FPH, Jia Liu, Wei Xue, Phy. Rev. Lett.126, 181102 (2021)

FPH, Chong Sheng Li, Phys.Rev. D96 (2017) no.9, 095028
FPH, Jianghao Yu, Phys.Rev.D 98 (2018) 9, 095022
Yan Wang, Chong Sheng Li, and FPH, Phys.Rev.D 104 (2021) 5, 053004
Ning Xie, FPH, arXiv:2207.11145 and work in progress

第十一届“威海新物理研讨会”@山东大学 威海 2022.08.05

Outline

- Research Motivation
- Explore ultra-light dark matter(DM) by SKA-like experiments and gravitational wave(GW) experiments
- Explore heavy DM by phase transition gravitational wave(GW)
- Conclusion

Motivation

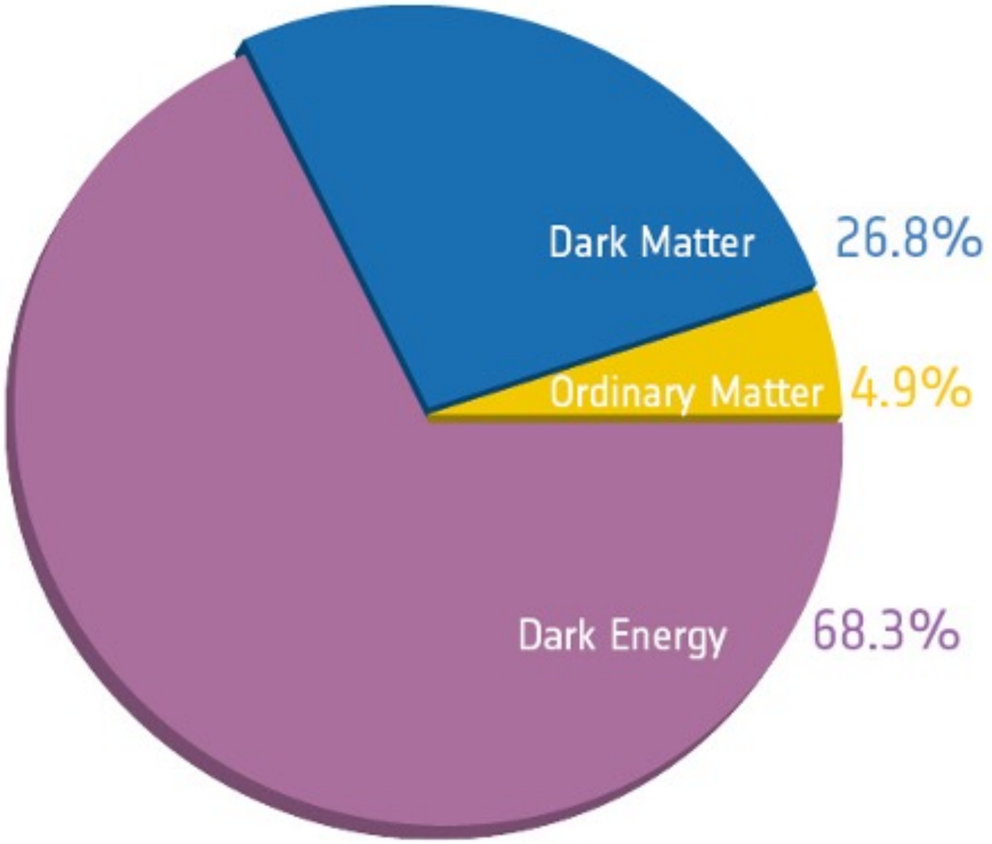

What is the nature of DM?

Many experiments have been done to unravel the long-standing problem.

However, no expected signals at LHC and DM direct search.

暗物质详细讨论见曹俊杰、安海鹏、王雯宇、汤勇老师的报告

希格斯粒子的发现@2012

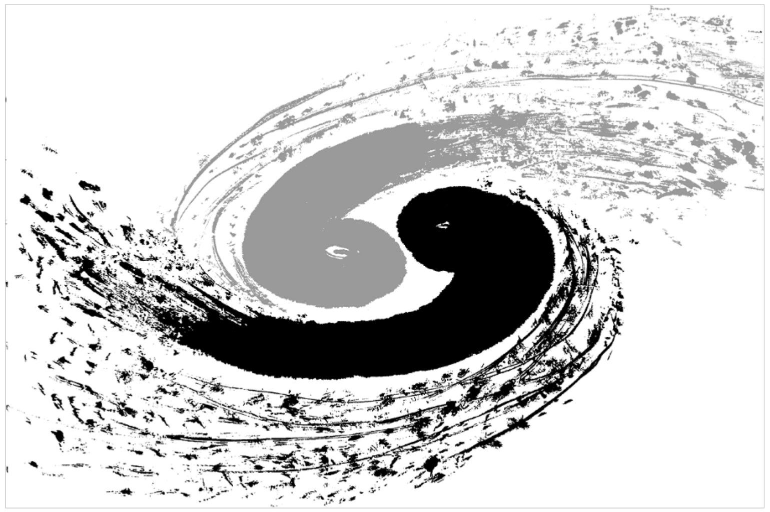

引力波的发现@2016

This situation may point us towards new ideas/approaches, such as

radio telescope (SKA/FAST),

gravitational wave (GW) detector (LISA/TianQin/Taiji)

What is dark matter?

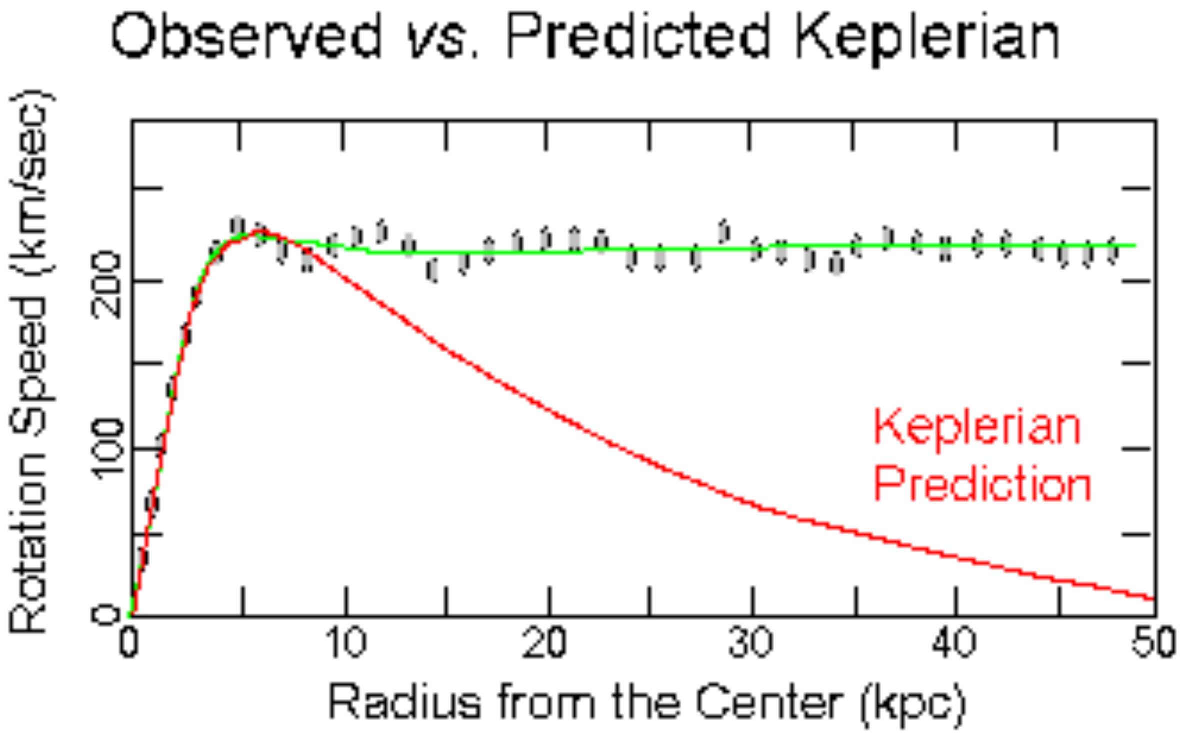

Galaxy rotation curve

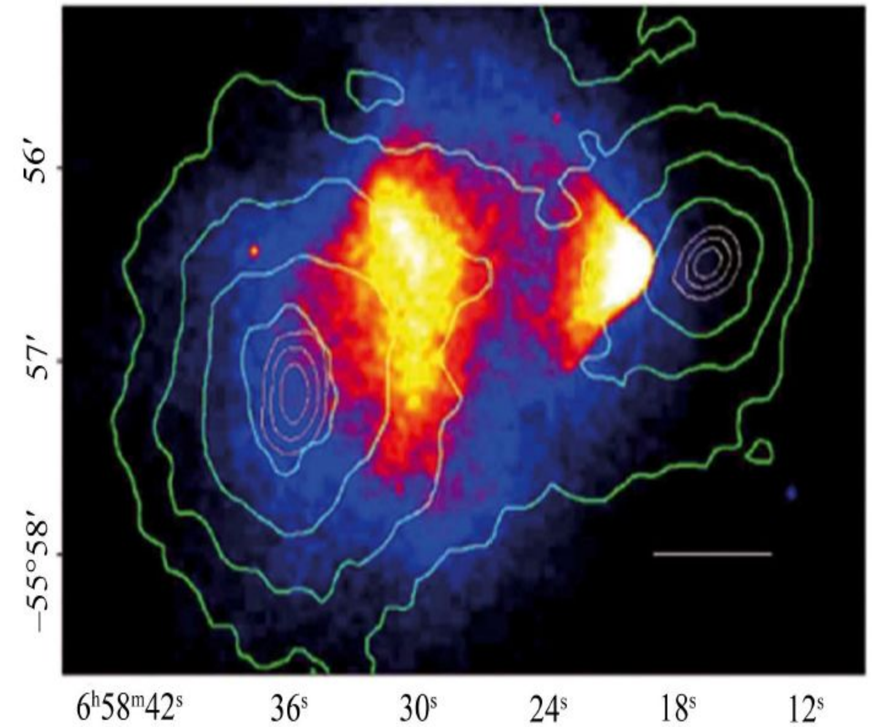

Bullet cluster collision

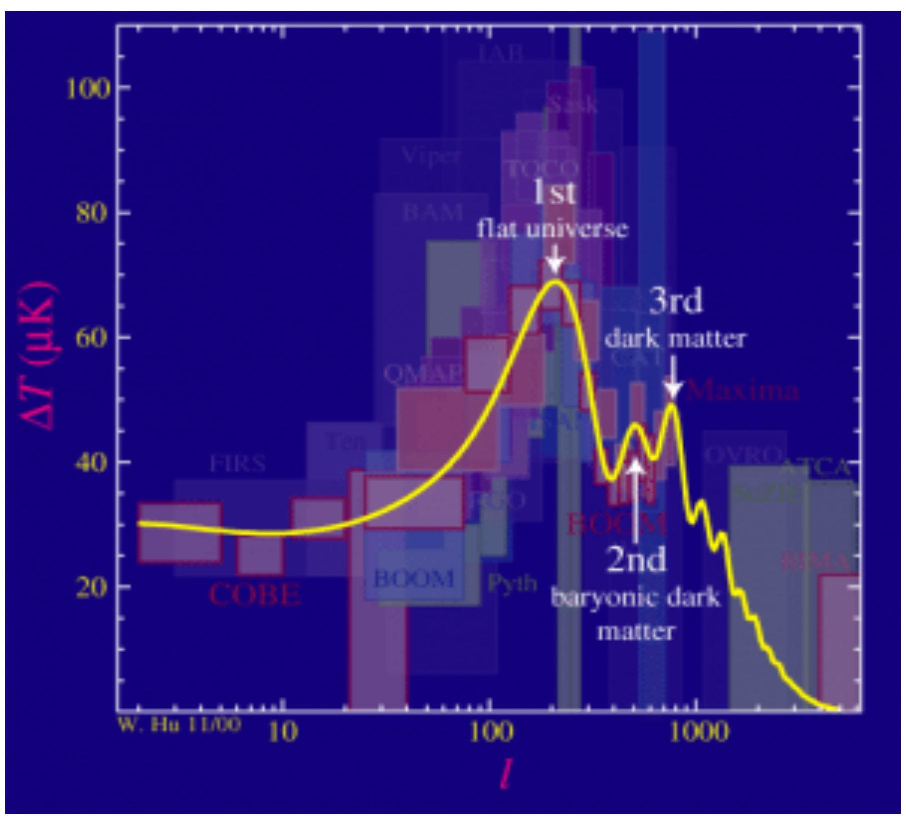

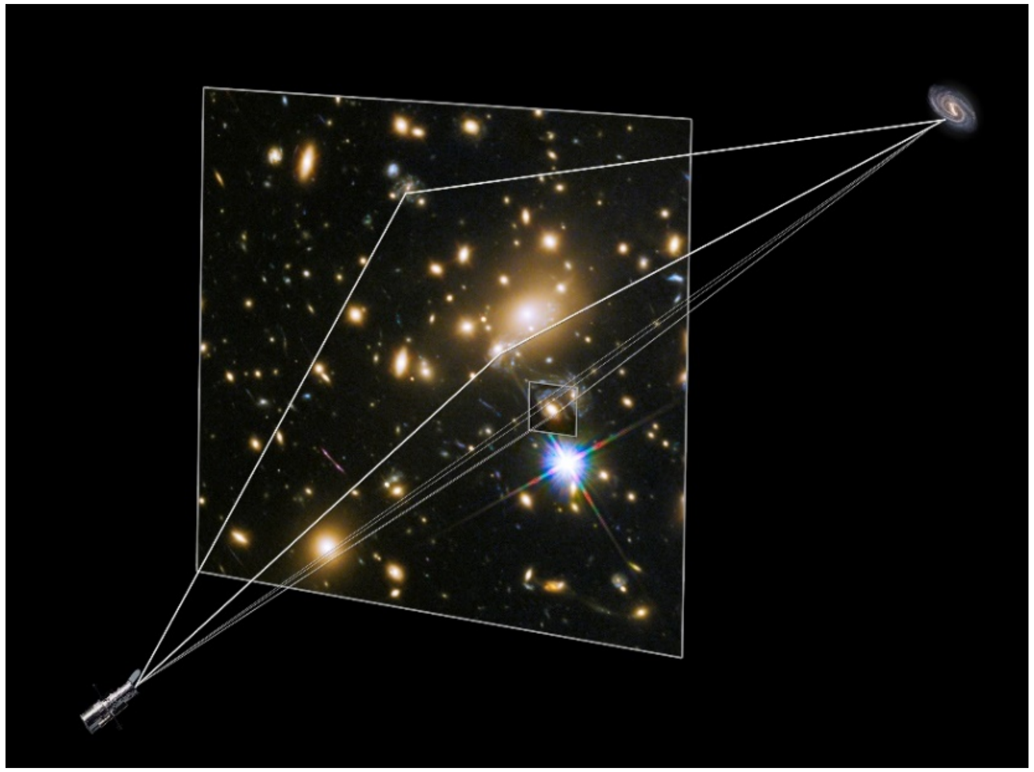

CMB spectrum

Gravitational lensing

What is GW?

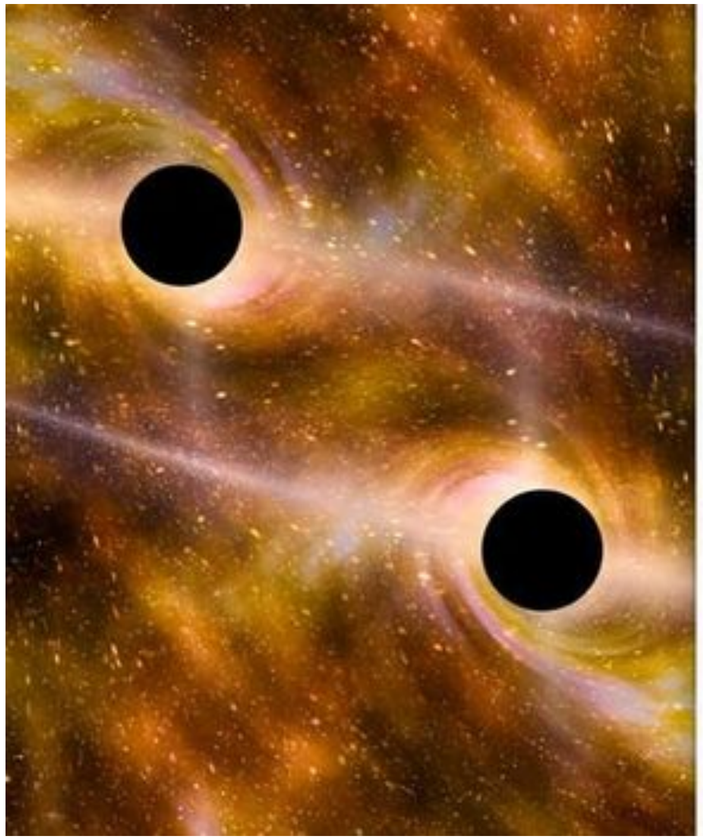

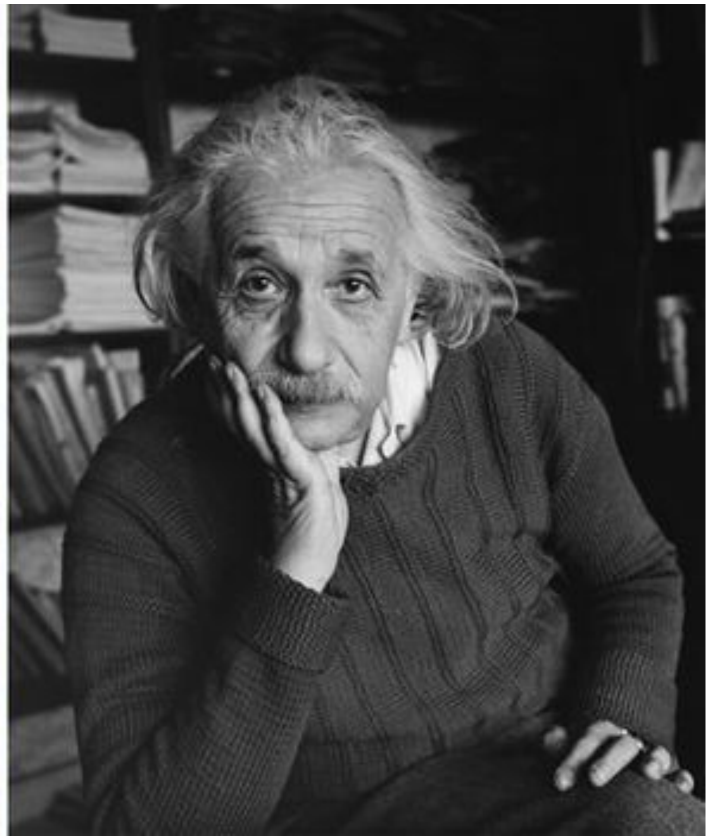

General relativity and Warped space time

$$R_{\mu\nu} - \frac{1}{2} R\, g_{\mu\nu} + \Lambda\, g_{\mu\nu} = \frac{8\pi G}{c^4} T_{\mu\nu}$$

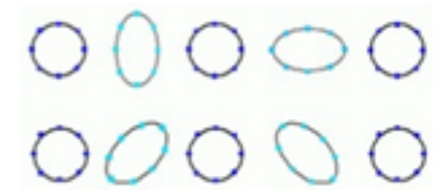

$$h_{ij} \simeq \frac{2G}{c^4 r} \ddot{Q}^{TT}_{ij}(t - r/c)$$

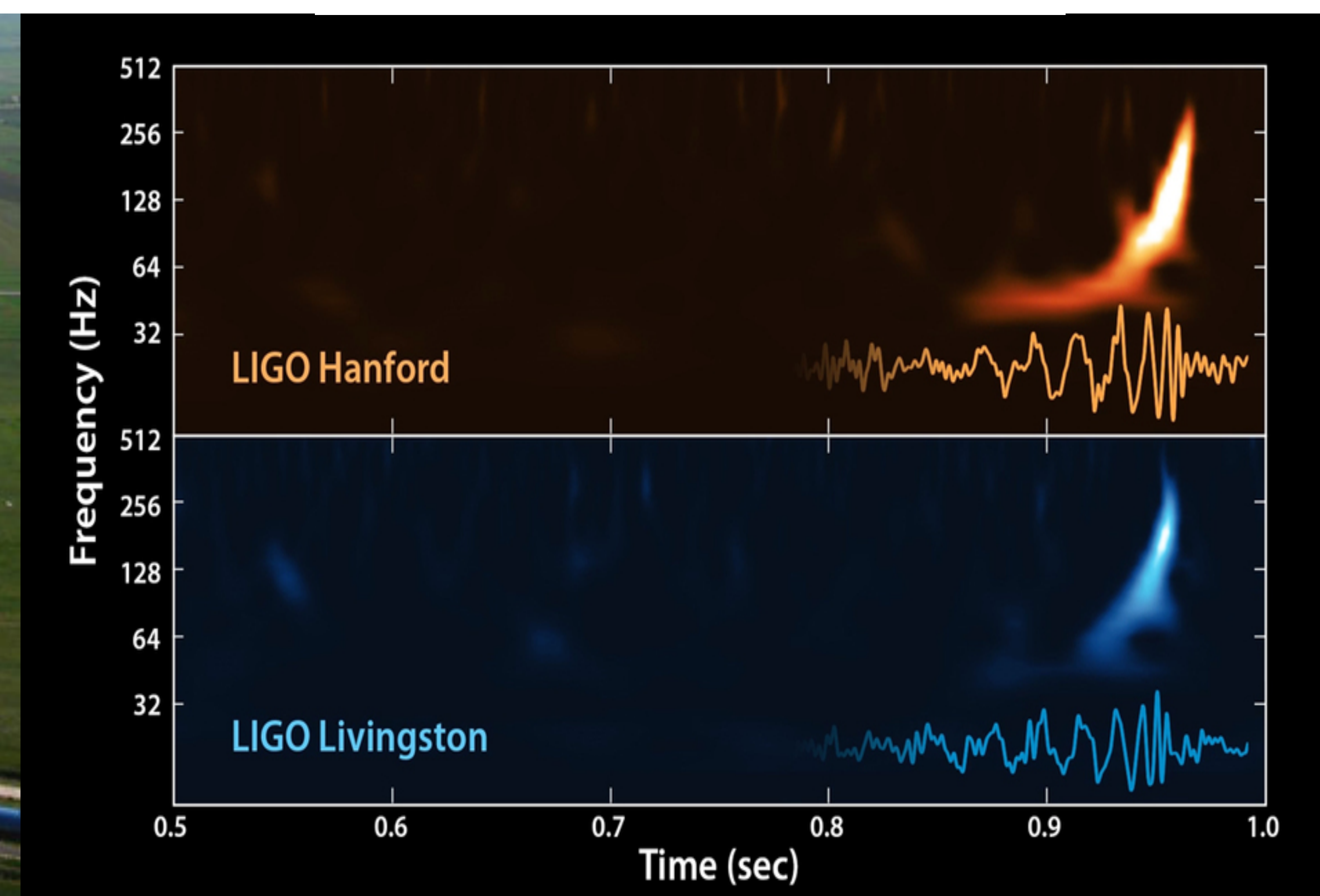

Motivation

LISA/TianQin/Taiji：
EW phase transition,
DM, baryogengesis

SKA, FAST, GBT(radio telescope)：
QCD phase transition,
Ultra-light DM

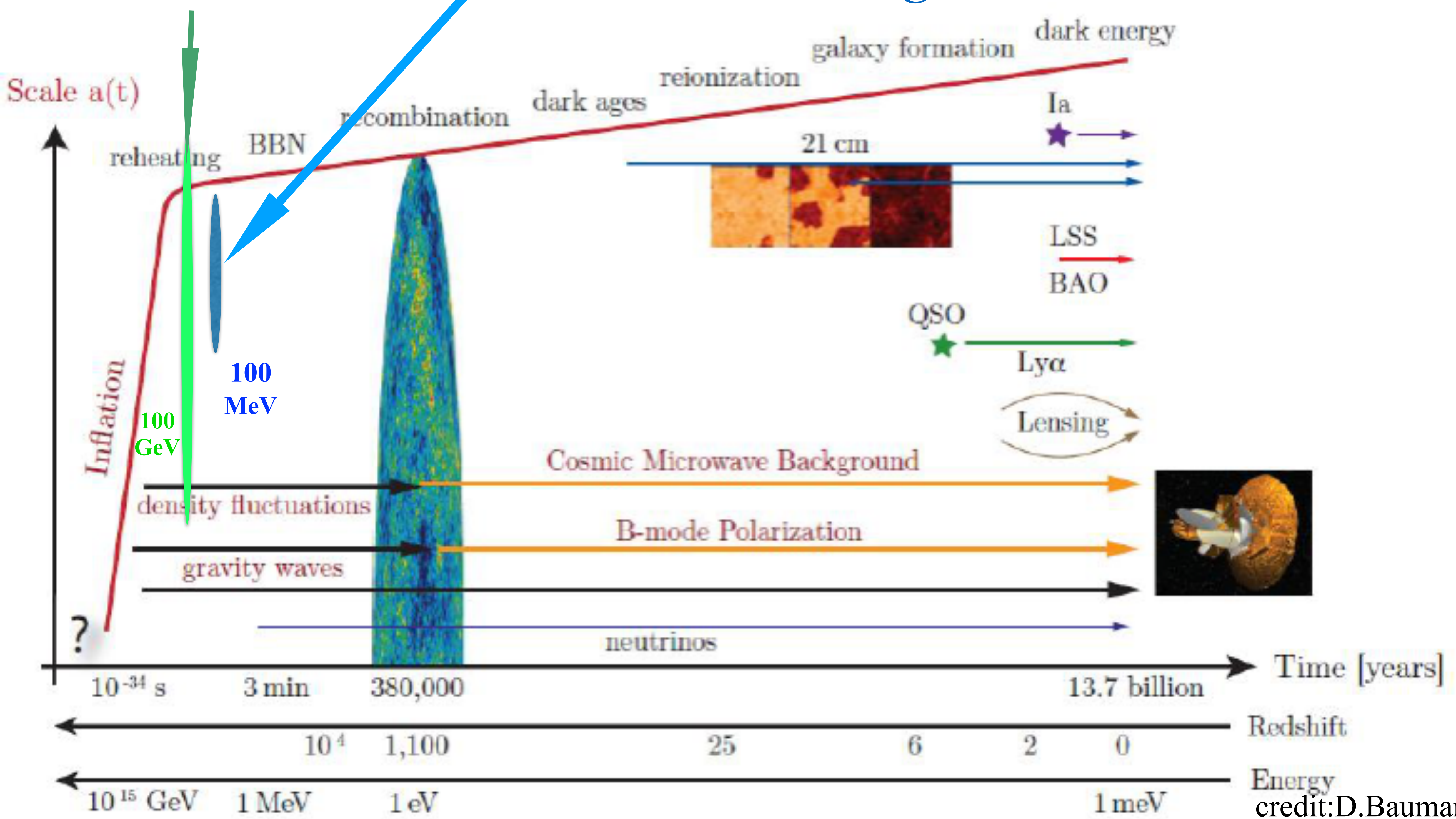

credit:D.Baumann

LISA: 2034 or earlier

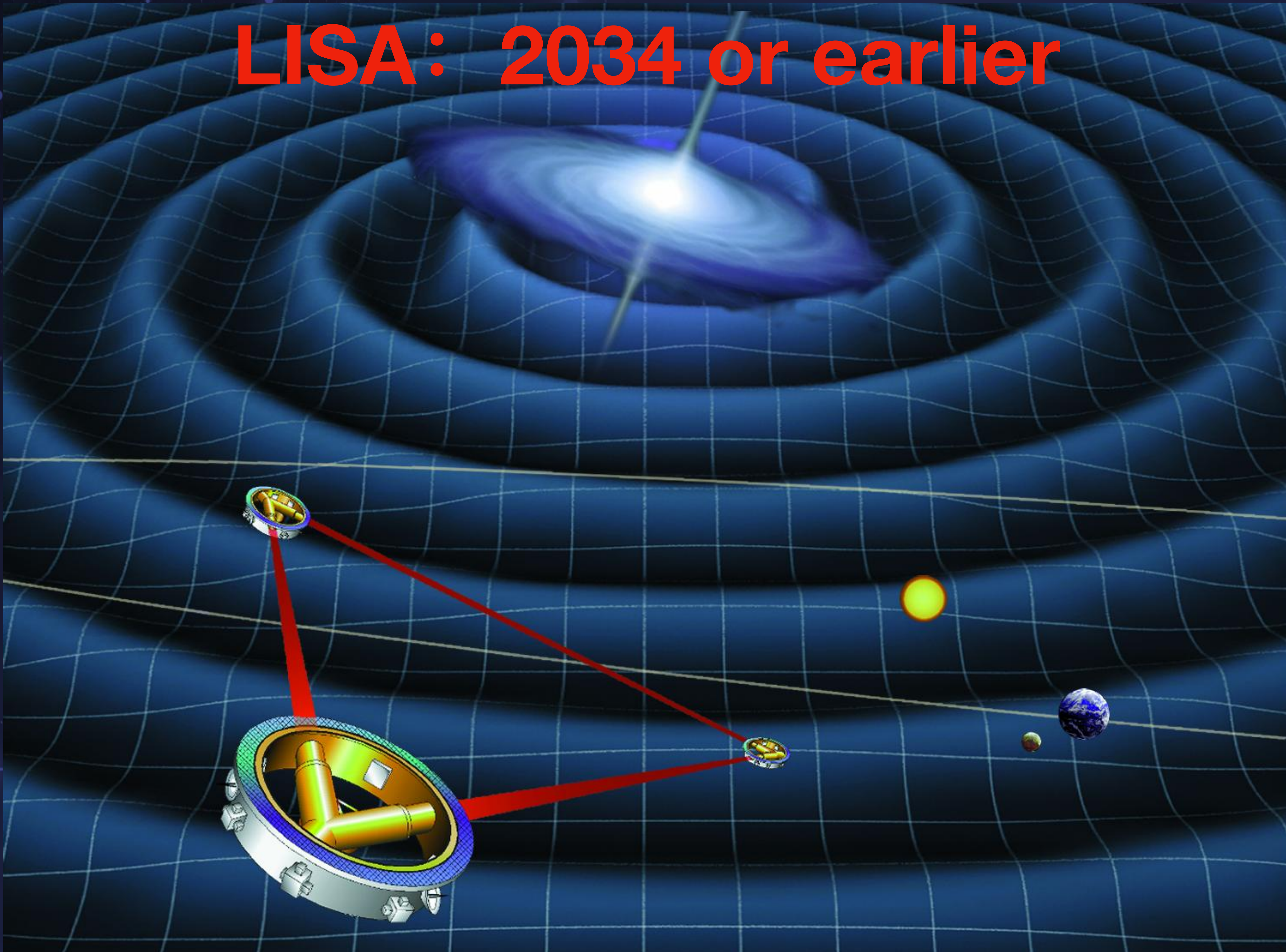

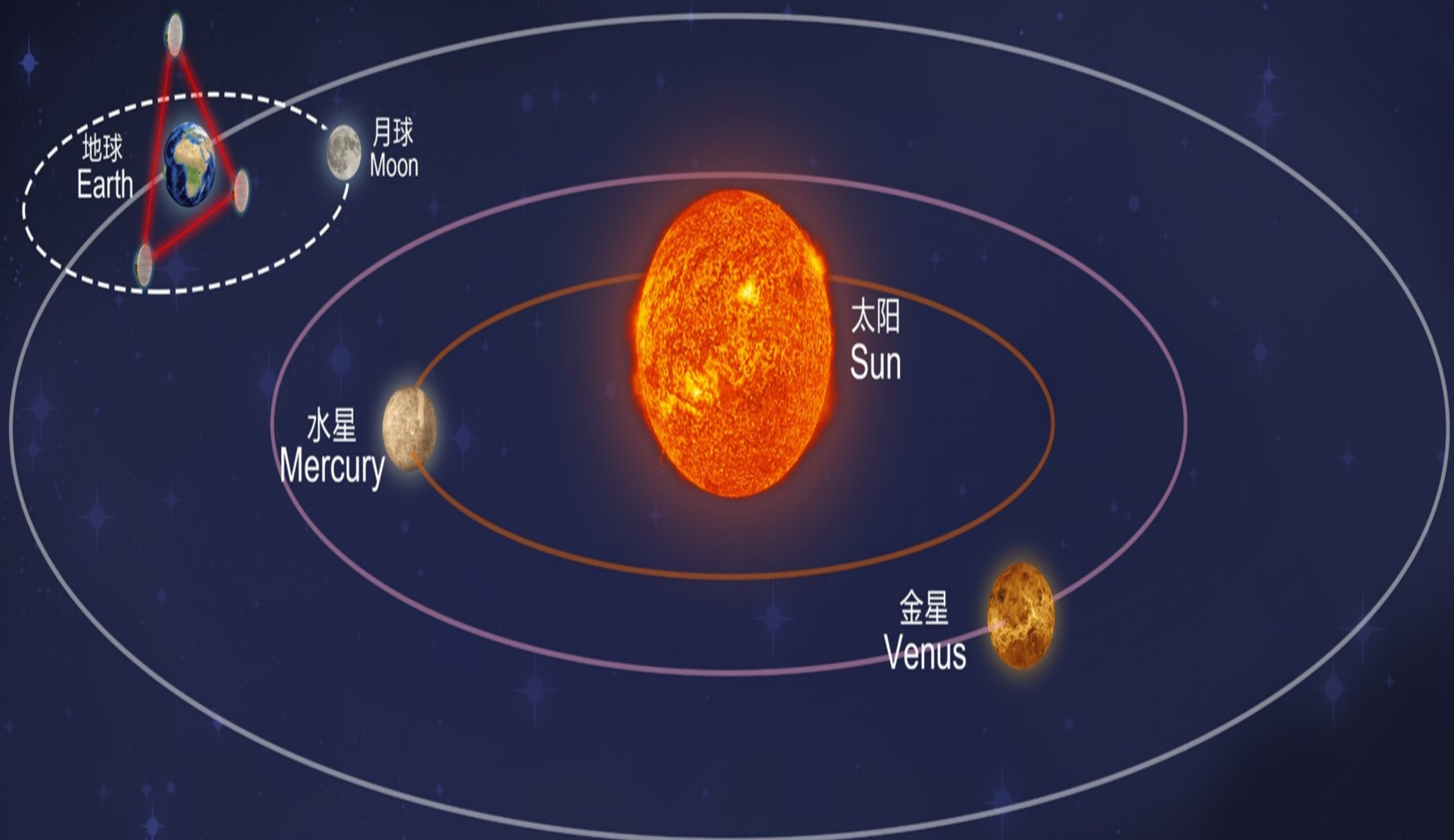

天琴

太极

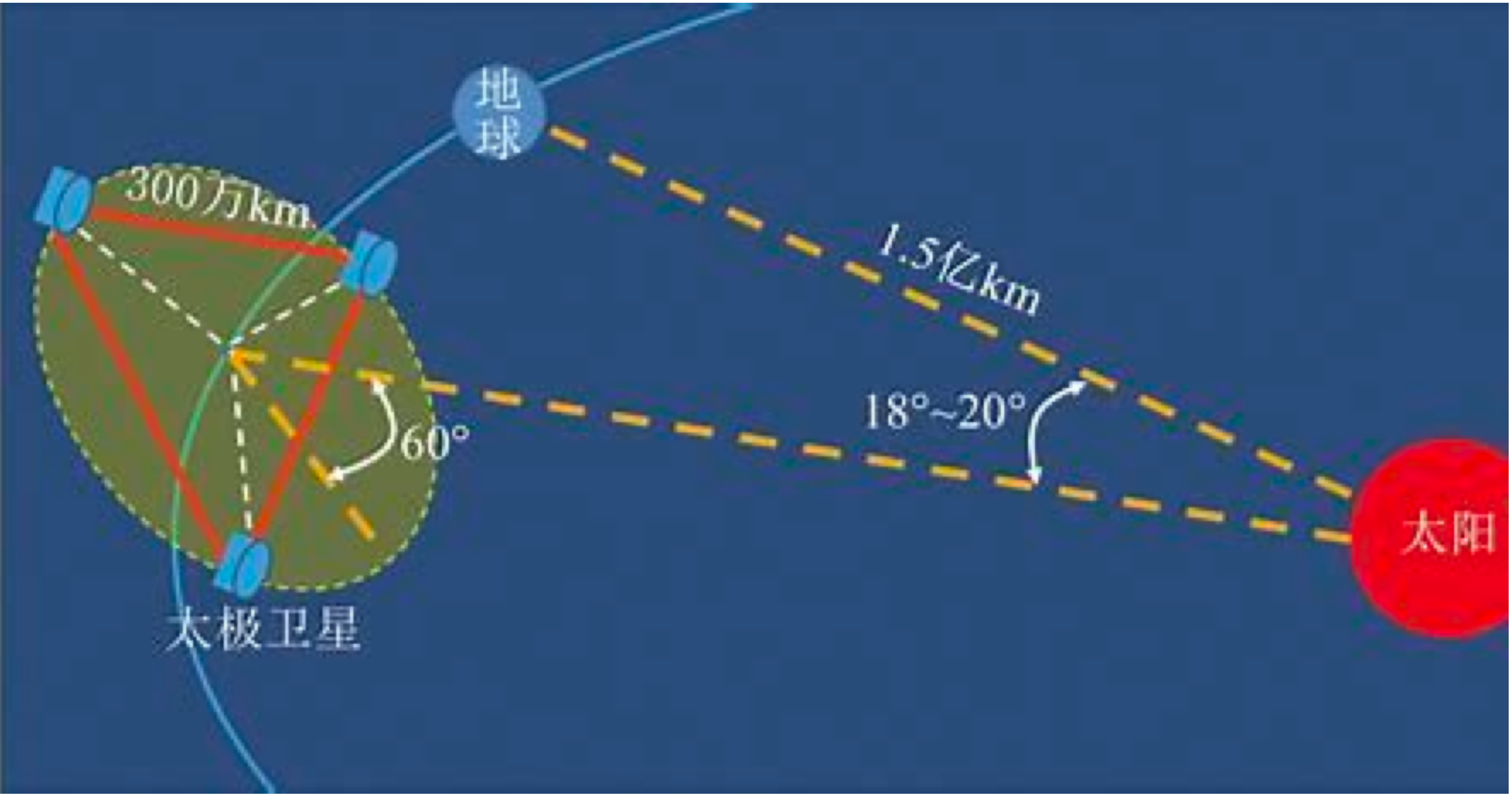

The Square Kilometre Array (SKA)详情见秦波老师报告

High sensitivity sub μJy

credit: SKA website

The Five-hundred-meter Aperture Spherical radio Telescope (FAST)

From 25 Sep. 2016

Credit:FAST website

The Green Bank Telescope (GBT)

GBT is running observations roughly 6,500 hours each year

credit:GBT website

超轻轴子暗物质的射电信号

Axion or axion-like particle motivated from strong CP problem or string theory is still one of the most attractive and promising DM candidate.

We firstly study using the SKA-like experiments to explore the resonant conversion of axion cold DM to radio signal from magnetized astrophysical sources, such as neutron star, magnetar and pulsar.

FPH, K. Kadota, T. Sekiguchi, H. Tashiro, Phys.Rev. D97 (2018) no.12, 123001, arXiv:1803.08230

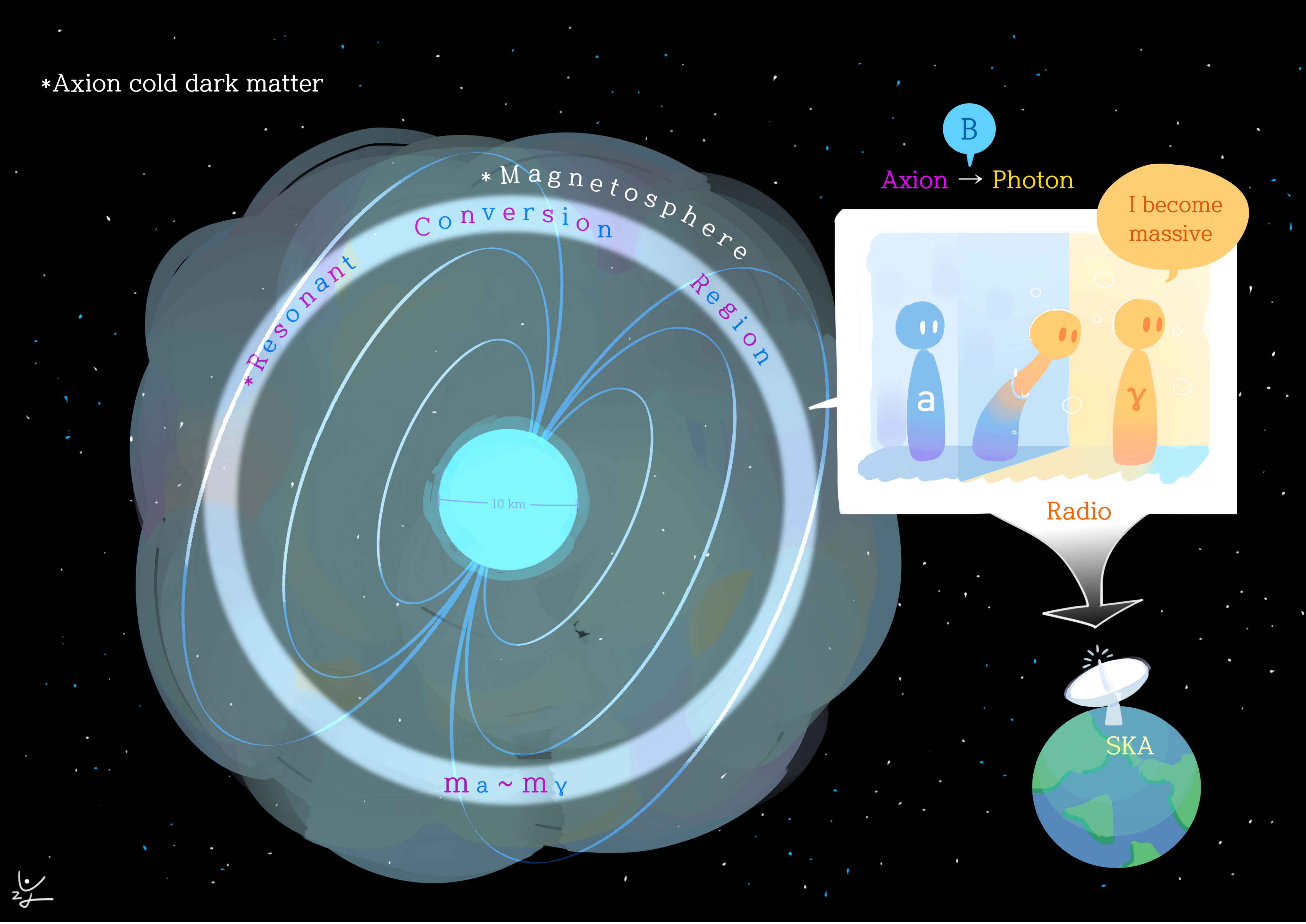

FPH, K. Kadota, T. Sekiguchi, H. Tashiro, Phys.Rev. D97 (2018) no.12, 123001

Radio telescope search for the resonant conversion of cold dark matter axions from the magnetized astrophysical sources

Three key points:

- **Cold DM is composed of non-relativistic axion or axion-like particles**

- **Neutron star (or pulsar and magnetar) has the strongest position-dependent magnetic field**

- **Neutron star is covered by magnetosphere and photon becomes massive therein**

Quick sketch of the neutron star size

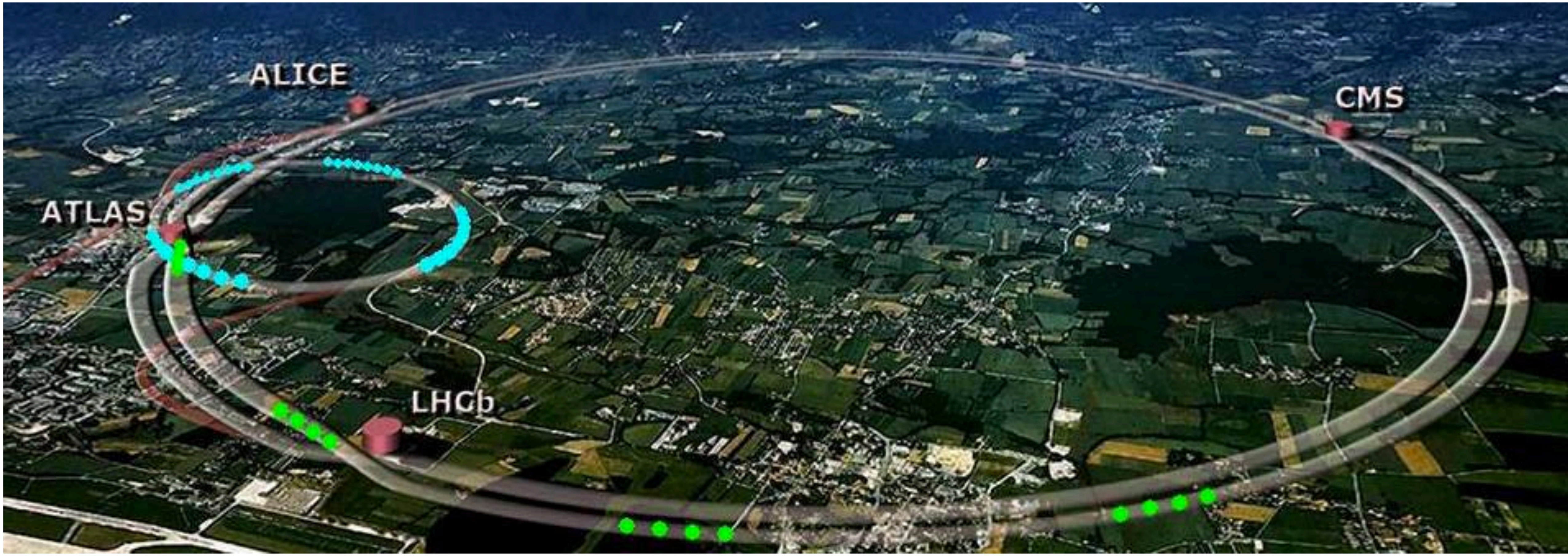

The radius of the neutron star is slightly larger than the radius of the LHC circle.

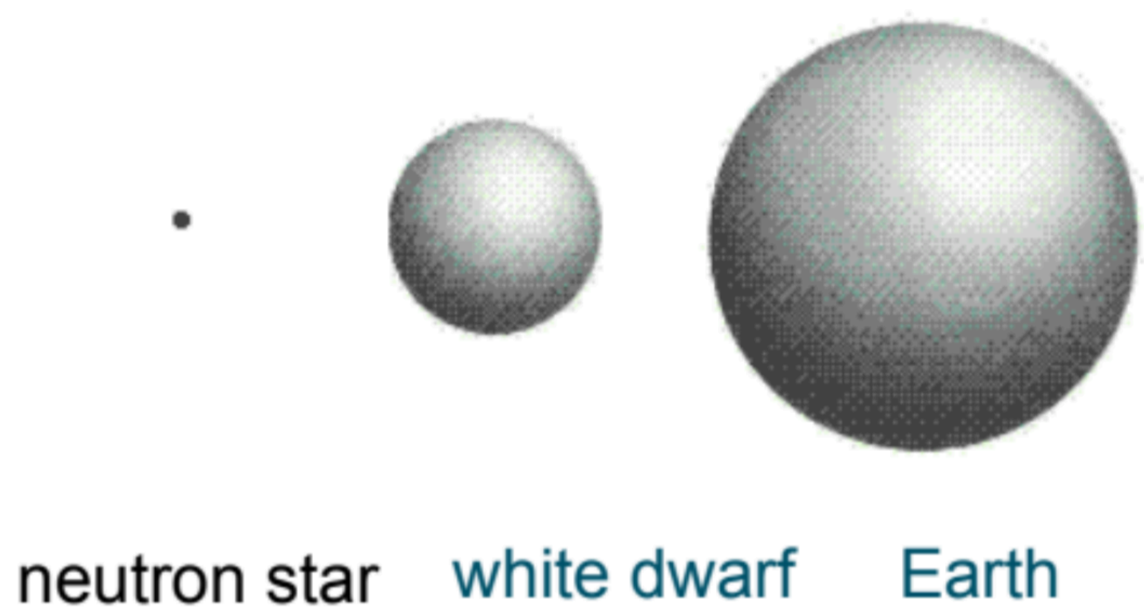

Strong magnetic field in the magnetosphere of Neutron star, Pulsar, Magnetar: the strongest magnetic field in the universe

1. **Mass:from 1 to 2 solar mass**

2. **Radius:** $r_0 \sim 10 - 20\text{km}$

3. **Strongest magnetic field**

$$B_0 \approx 10^{12} - 10^{15}\text{G}$$

$$B_0 \sim 3.3 \times 10^{19}\sqrt{P\dot{P}} \quad \text{G}$$

4. **Neutron star is surrounded by large region of magnetosphere, where photon becomes massive.**

$$r \sim 100 r_0$$

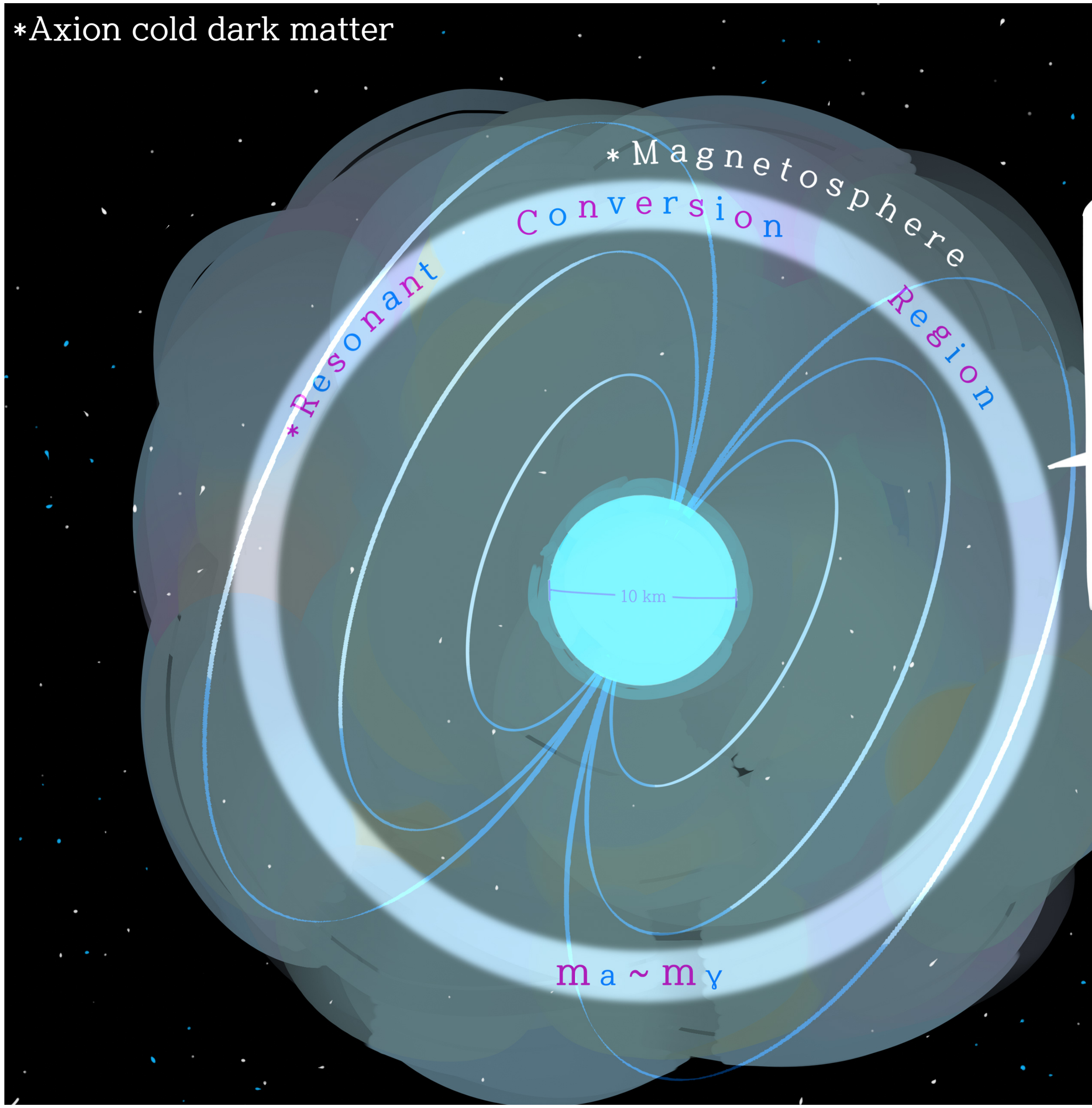

Axion-photon conversion in the magnetosphere

$$L_{\text{int}} = \frac{1}{4} g \tilde{F}^{\mu\nu} F_{\mu\nu} a = -g \mathbf{E} \cdot \mathbf{B} a,$$

Massive Photon: In the magnetosphere of the neutron star, photon obtains effective mass in the plasma.

$$m_\gamma^2 = \omega_{plasma}^2 = 4\pi\alpha \frac{n_e}{m_e}$$

$$n_e(r) = n_e^{\rm GJ}(r) = 7 \times 10^{-2} \frac{1s}{P} \frac{B(r)}{1\ \rm G} \frac{1}{\rm cm^3}$$

$$B(r) = B_0 \left(\frac{r}{r_0}\right)^{-3}$$

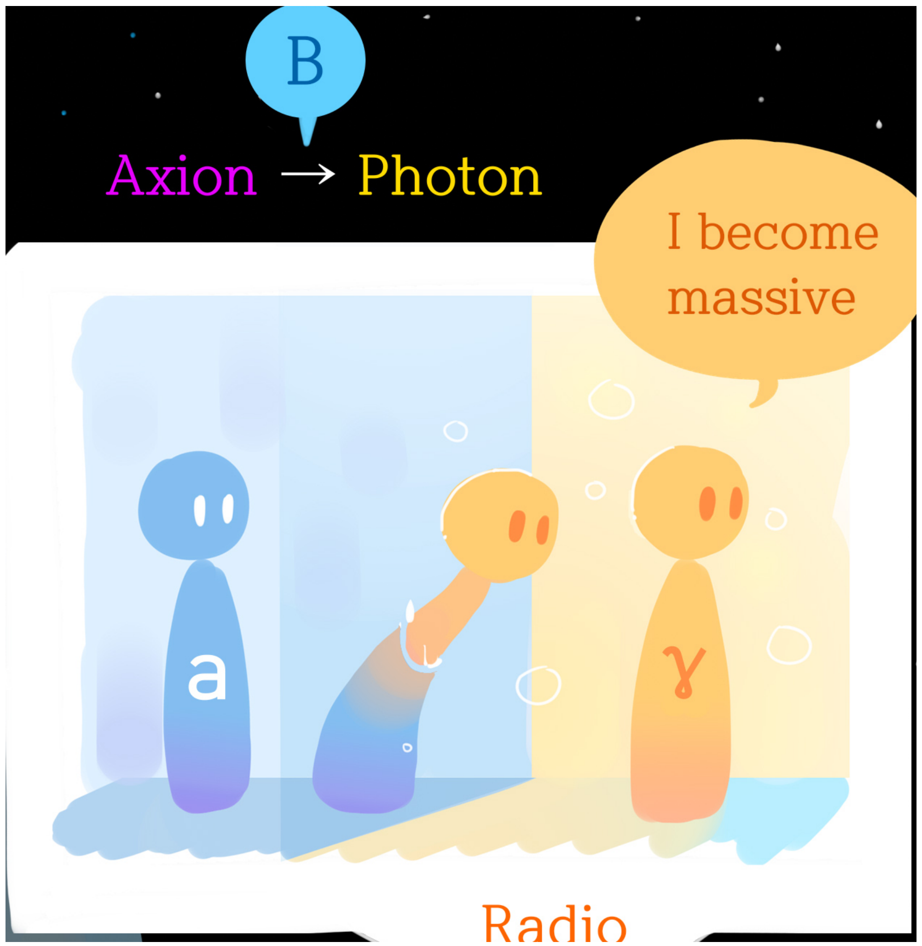

Thus, the photon mass is location dependent, and within some region

$$m_\gamma^2(r_{\rm res}) = m_a^2$$

- G. Raffelt and L. Stodolsky, Phys. Rev. D 37, 1237 (1988)

The Adiabatic Resonant Conversion

Like MSW effects

$$\left[\omega^2 + \partial_z^2 + \begin{pmatrix} -m_\gamma^2 & gB\omega \\ gB\omega & -m_a^2 \end{pmatrix}\right]\begin{pmatrix} \gamma \\ a \end{pmatrix} = 0,$$

$$\sin 2\tilde{\theta} = \frac{2gB\omega}{\sqrt{4g^2B^2\omega^2 + (m_\gamma^2 - m_a^2)^2}} \qquad m_\gamma^2(r_{\mathrm{res}}) = m_a^2$$

within resonance region, the conversion rate is greatly enhanced due to resonant effects.

The adiabatic resonant conversion requires the resonance region is valid inside the resonance width.

Radio Signal

Line-like radio signal for non-relativistic axion conversion:

$$\nu_{\rm peak} \approx \frac{m_a}{2\pi} \approx 240\frac{m_a}{\mu eV}{\rm MHz}$$

1 GHz ~ 4 μeV

FAST:70MHz–3GHz, SKA:50MHz–14GHz, GBT:0.3–100GHz

Radio telescopes can probe axion mass of 0.2–400 μeV

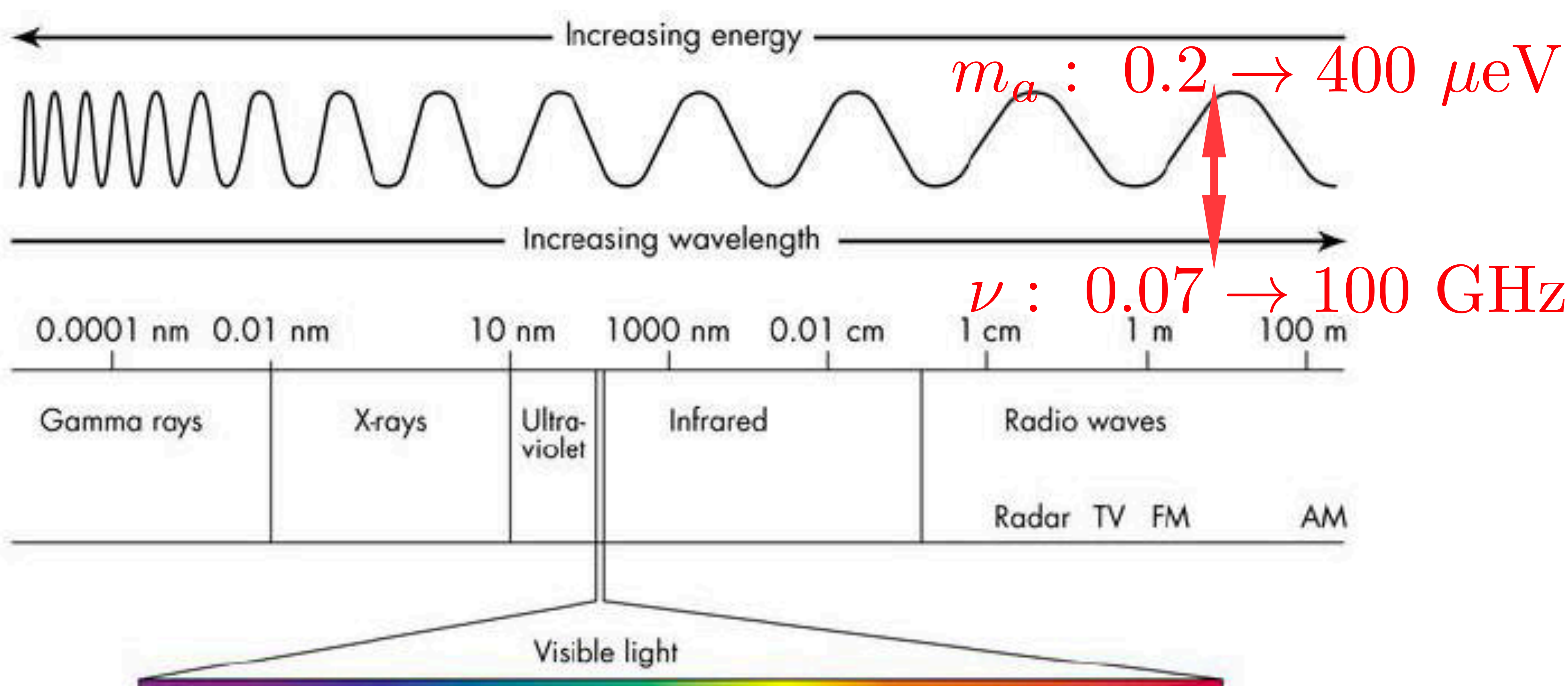

Radio Signal

Signal: For a trial parameter set, $B_0 = 10^{15}$ G, $m_a = 50\ \mu$eV

$P = 10$ s, $g = 5 \times 10^{-11}$ GeV^{-1}, $r_0 = 10$ km, $M = 1.5 M_{\rm sun}$, $d = 1$kpc

$S_\gamma \sim 0.51\ \mu$Jy.

Sensitivity: $S_{\rm min} \sim 0.48 \mu Jy$ for the SKA1

$S_{min} \sim 0.016 \mu Jy$ for SKA2 with 100 hours observation time.

SKA-like experiment can probe the axion DM and the axion mass which corresponds to peak frequency.

Working in progress on more delicate study.

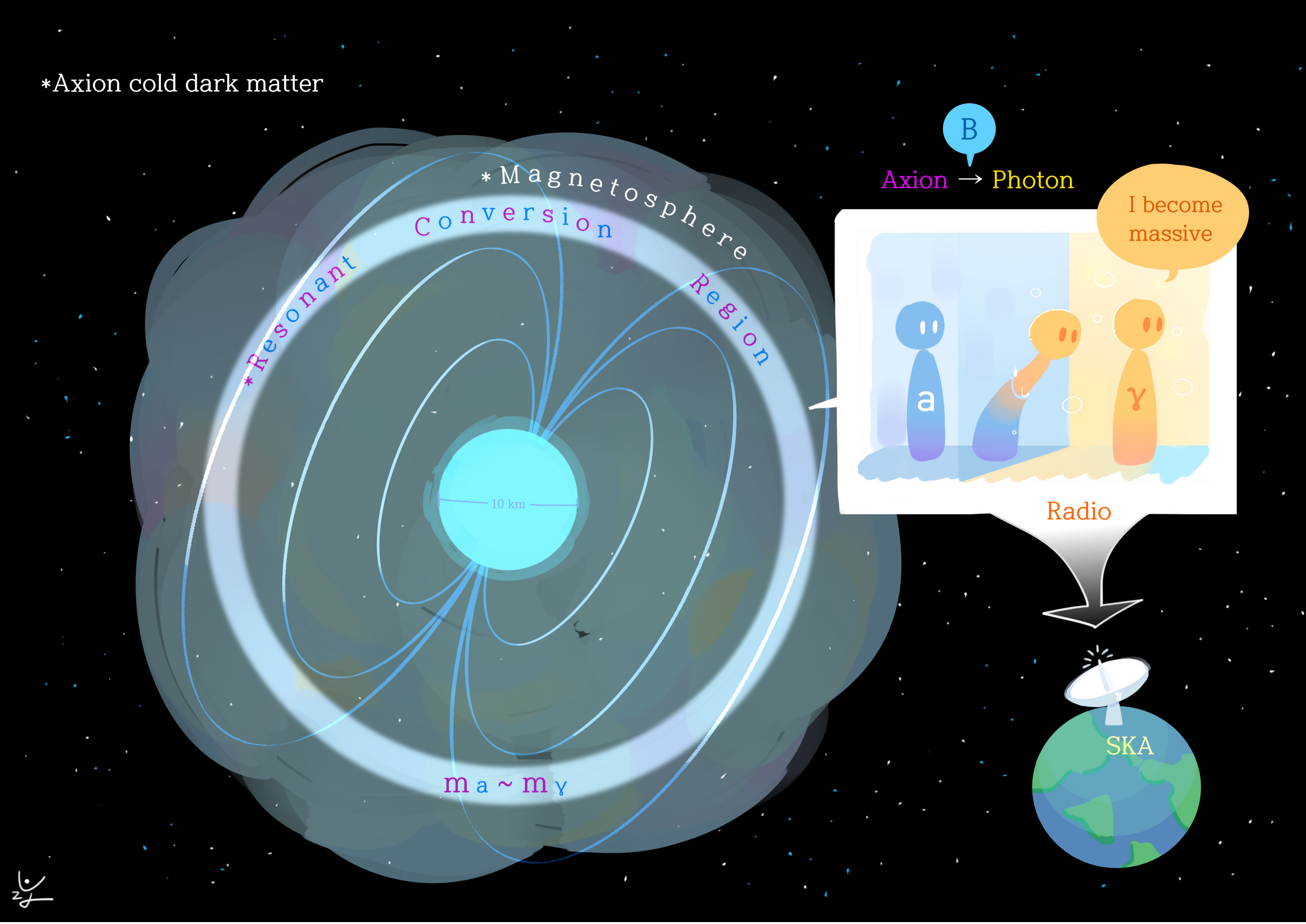

FPH, K. Kadota, T. Sekiguchi, H. Tashiro, Phys.Rev. D97 (2018) no.12, 123001

Comments on the radio probe of axion DM

1. **Astrophysical uncertainties:the magnetic field distribution, DM density distribution, the velocity dispersion, the plasma effects…**

2. **There are more and more detailed studies after our simple estimation on the radio signal:**

arXiv:1804.03145 They consider more details and extremely high dark matter density around the neutron star, thus the signal is more stronger.

arXiv:1811.01020 by Benjamin R. Safdi, Zhiquan Sun, Alexander Y. Chen

arXiv:1905.04686,They consider multi-messenger of axion DM detection. Namely, using LISA to detect the DM density around the neutron star, which can determine the radio strength detected by SKA.

A precise study is arXiv:2104.08290

***Xiao-Jun Bi, et. al.* *Phys.Rev.D* 104 (2021) 10, 103015， *Phys.Rev.D* 103 (2021) 11, 115021**

探测暗物质的热门新方法

FPH, **K. Kadota, T. Sekiguchi, H. Tashiro, Phys.Rev. D97 (2018) no.12, 123001, arXiv:1803.08230, Cited by 63 times**

该新方法现实可行，快速成为探测暗物质的热门新方法，为**SKA**和**FAST**提供了新的物理研究动机, 同时也能促进引力波多信使研究。 更多的综合性讨论如下：

✓欧洲粒子物理**2020**战略报告中单列一节介绍该新方法：**Physics Briefing Book : Input for the European Strategy for Particle Physics Update 2020, section 9.5.3[arXiv:1910.11775]**

✓**2021**年欧洲粒子天体理论联盟白皮书**(EuCAPT)**也列举了该新方法 **[arXiv:2110.10074]**

✓**Pierre Sikivie**教授介绍寻找轴子方法的综述 **Rev.Mod.Phys.93(2021)1,015004**，单列一段介绍该新方法

✓2022 年 3 月最新的 Snowmass Summer 两篇综述都 arXiv:2203.06380, arXiv: 2203.07984 介绍了该新方法。

Generalization to axion star case

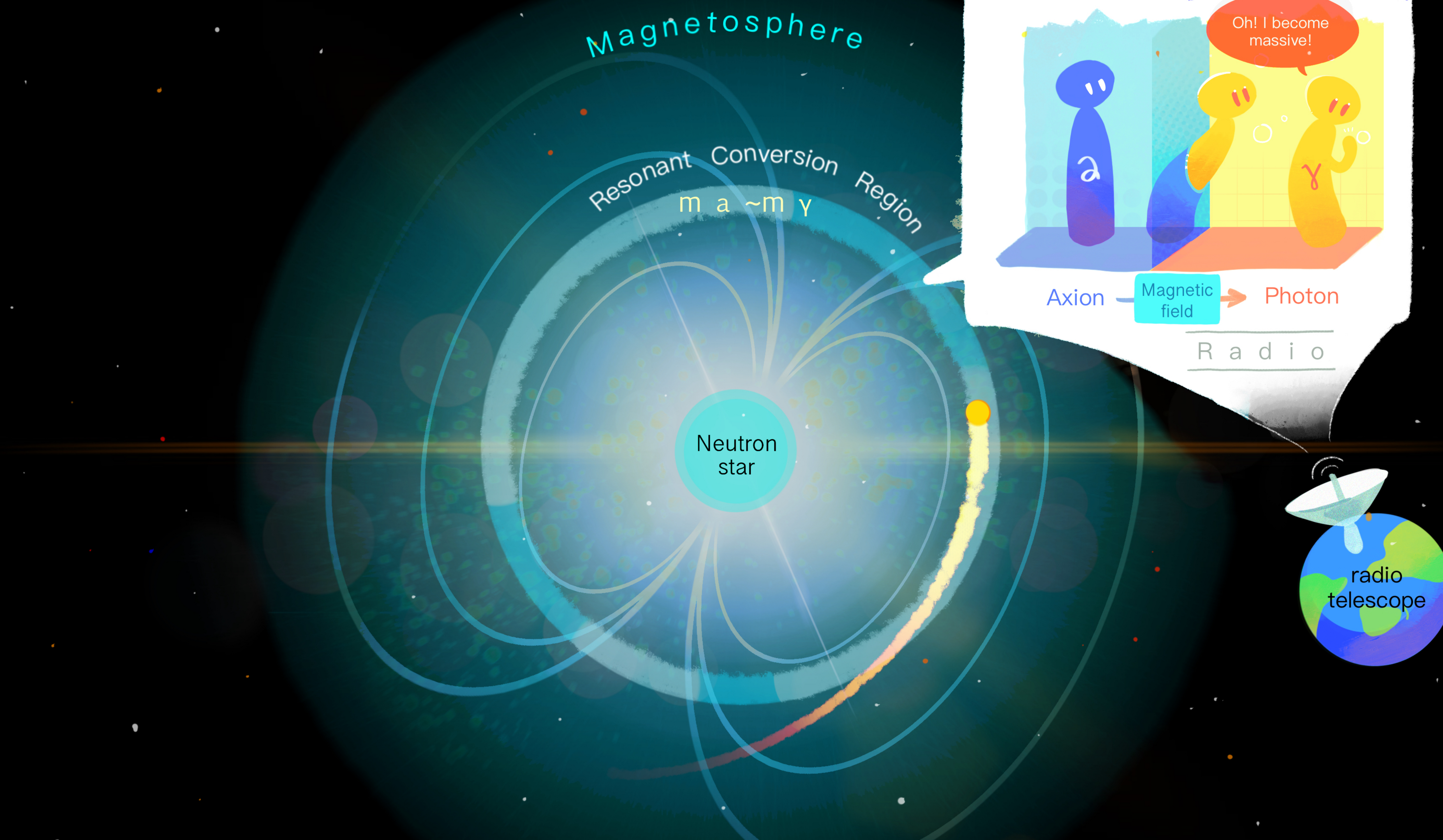

用轴子凝聚产生的轴子星在磁星磁层内的共振效应来解释快速射电暴(FRB)的起源

James Buckley, Bhupal Dev, Francesc Ferrer, FPH, *Phys.Rev.D* 103 (2021) 4, 043015

Mysterious Fast Radio Bursts (FRBs)

Recently, FRBs become the most mysterious phenomenon in astrophysics and cosmology (D. Thornton, et al., (2013) Science, 341, 53)**.**
FRBs are intense, transient radio signals with large dispersion measure. However, their origin and physical nature are still obscure.

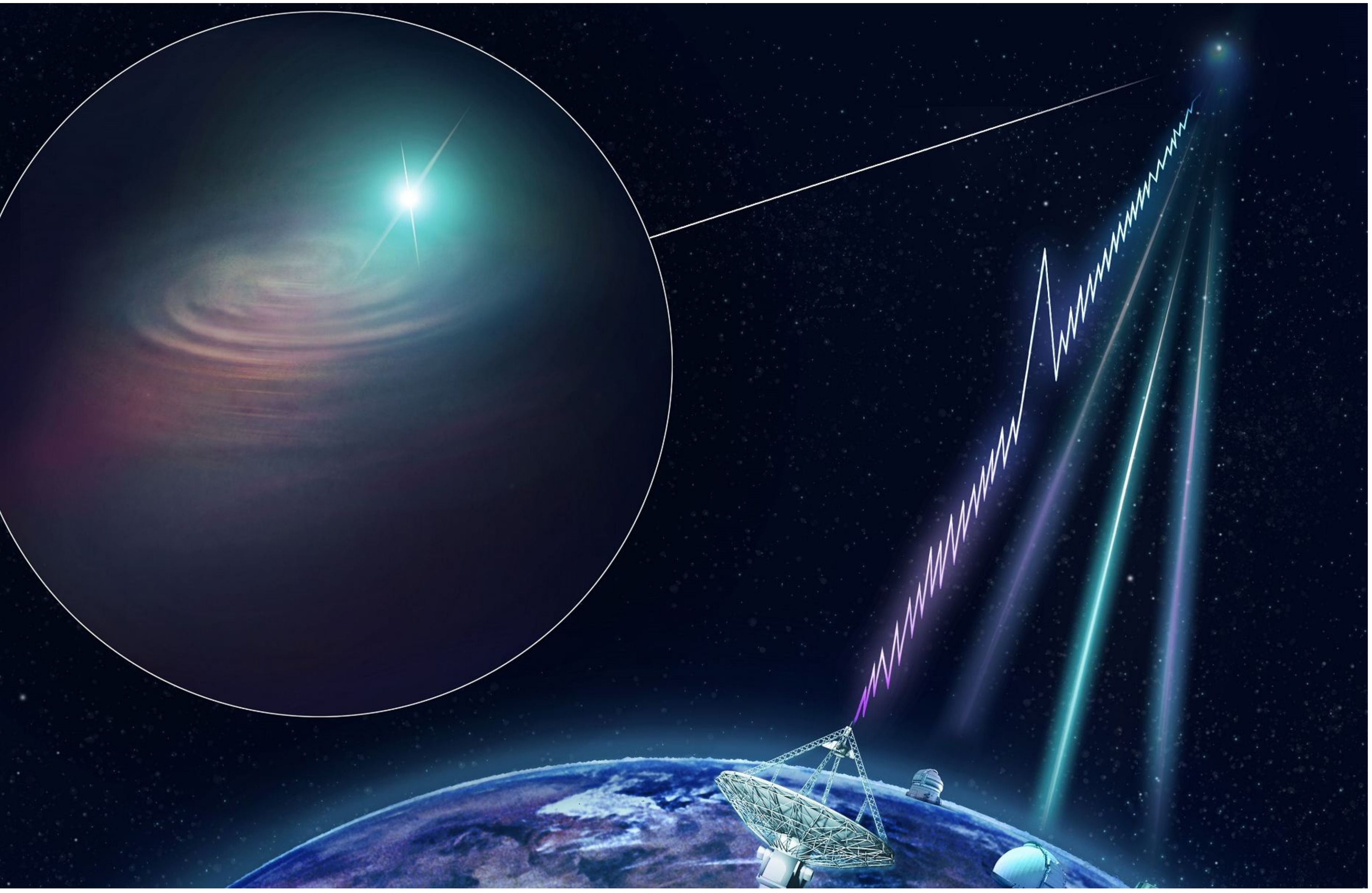

$\mathcal{O}(0.1)$ to $\mathcal{O}(100)$ Jy

$\mathcal{O}(10^{38})$ to $\mathcal{O}(10^{40})$ erg

Duration: milliseconds

$$0.1 \lesssim z \lesssim 2.2$$

Focus on FRBs events with from 800 MHz to 1.4 GHz by Parkes, ASKAP, and UTMOST.

From Universe Today

FRB-Axion star correlation

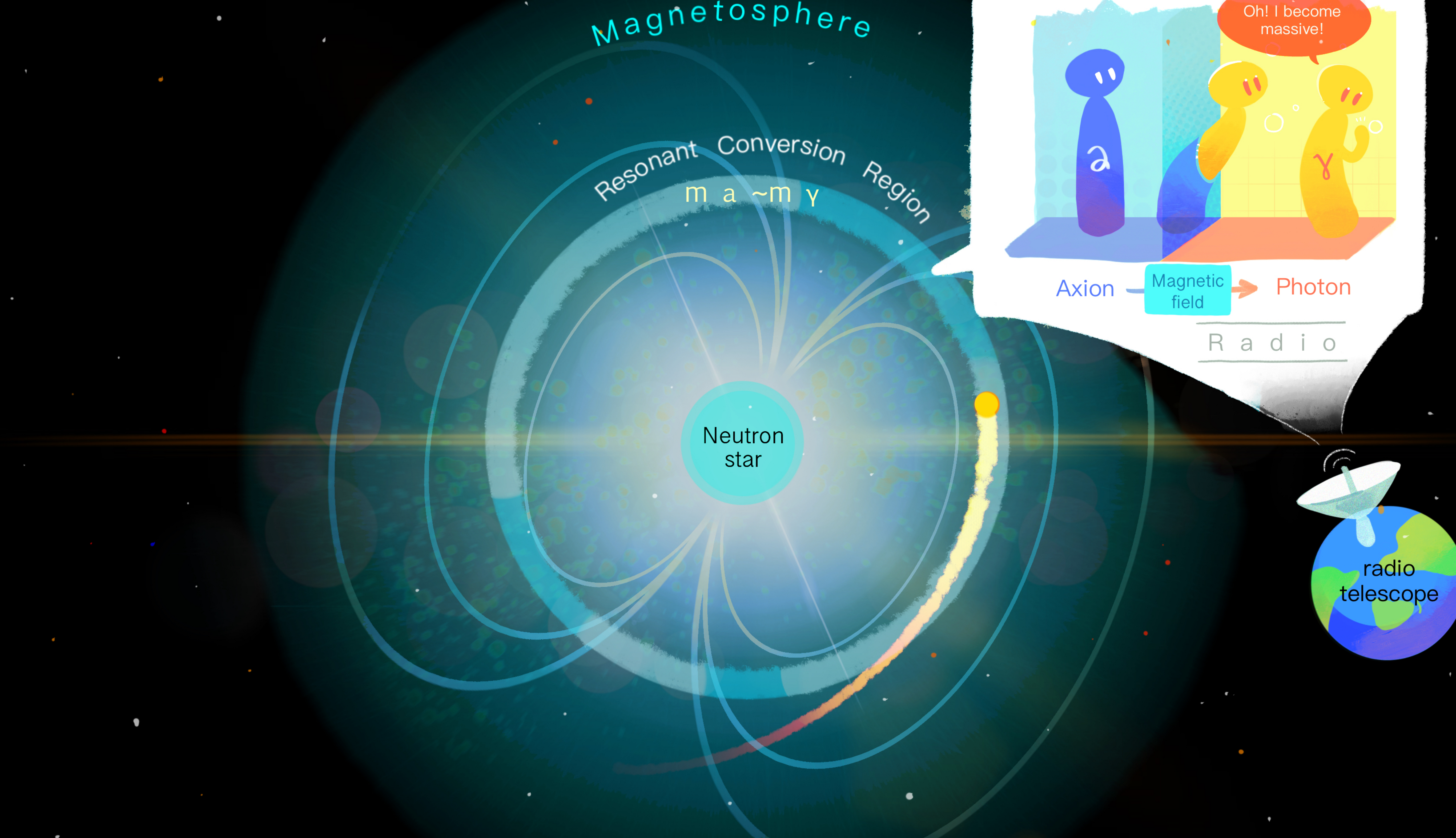

用轴子凝聚产生的轴子星在磁星的磁层内的共振效应来解释快速射电暴(FRB)的起源

James Buckley, Bhupal Dev, Francesc Ferrer, FPH, *Phys.Rev.D* 103 (2021) 4, 043015

Generalize to dark photon DM case

Haipeng An, FPH, Jia Liu, Wei Xue, Phy. Rev. Lett.126, 181102 (2021)

Recently, people realize light dark photon can be a promising DM candidate.

P. W. Graham, J. Mardon, and S. Rajendran, Phys. Rev. D 93, 103520 (2016).
A.J. Long and L.-T. Wang, Phys. Rev. D 99, 063529 (2019)
B. G. Alonso-Álvarez, T. Hugle, and J. Jaeckel, J. Cosmol. Astropart. Phys. 02 (2020) 014.
C. K. Nakayama, J. Cosmol. Astropart. Phys. 10 (2019) 019.
P. Agrawal, N. Kitajima, M. Reece, T. Sekiguchi, and F. Takahashi, Phys. Lett. B 801, 135136 (2020).
R. T. Co, A. Pierce, Z. Zhang, and Y. Zhao, Phys. Rev. D 99, 075002 (2019).
D. Y. Nakai, R. Namba, and Z. Wang, J. High Energy Phys. 12 (2020) 170

We study how to detect light dark photon DM by radio telescope, following the same idea as the axion DM case.

$$\mathcal{L} = -\frac{1}{4}F'_{\mu\nu}F'^{\mu\nu} - \frac{1}{2}m_{A'}^2 A'_\mu A'^\mu - \frac{1}{2}\epsilon F_{\mu\nu}F'^{\mu\nu}$$

Resonant conversion process

Haipeng An, FPH, Jia Liu, Wei Xue, Phy. Rev. Lett.126, 181102 (2021)

更一般性的讨论见安海鹏老师的报告。

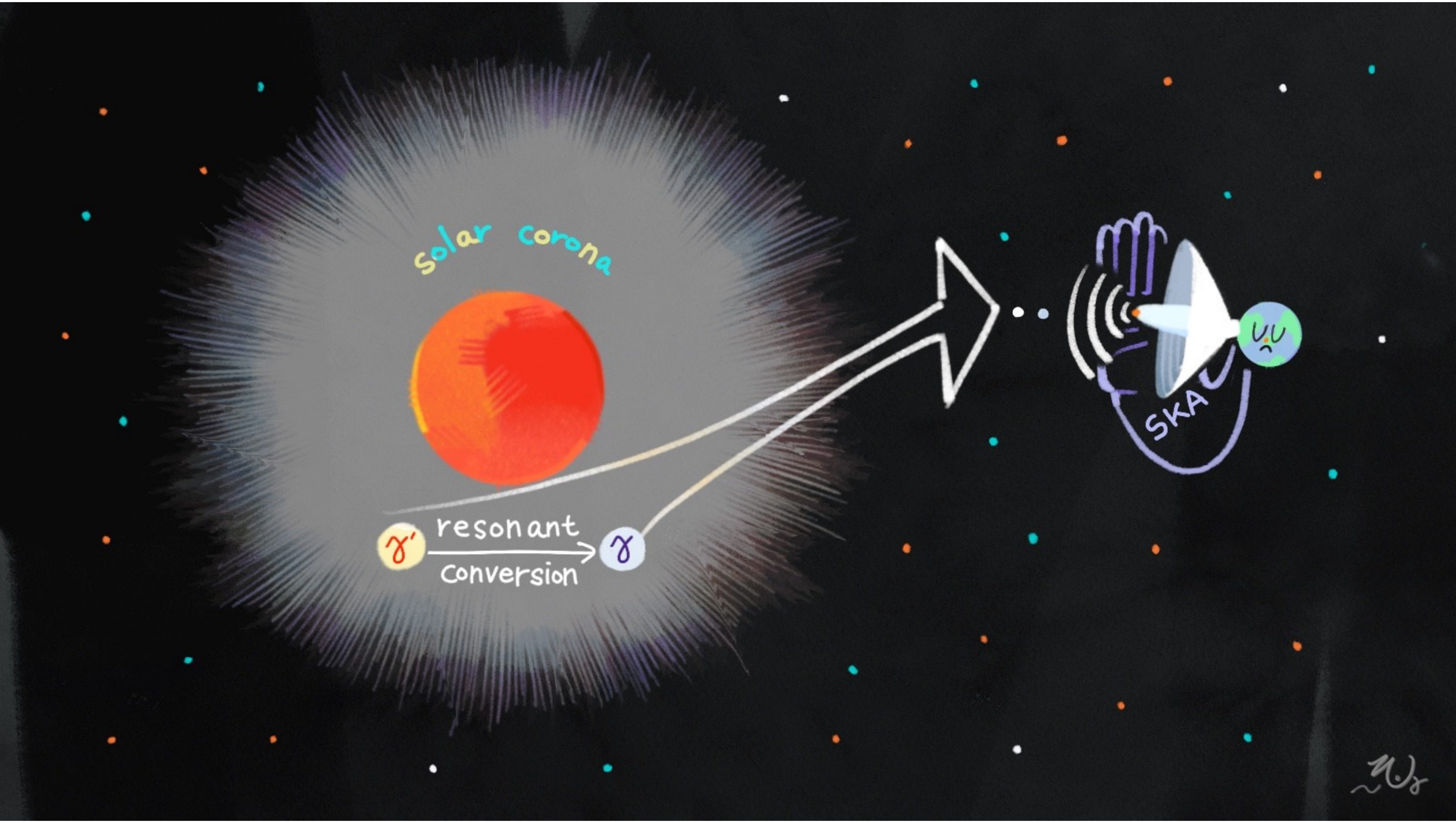

Generalisation to dark photon DM case

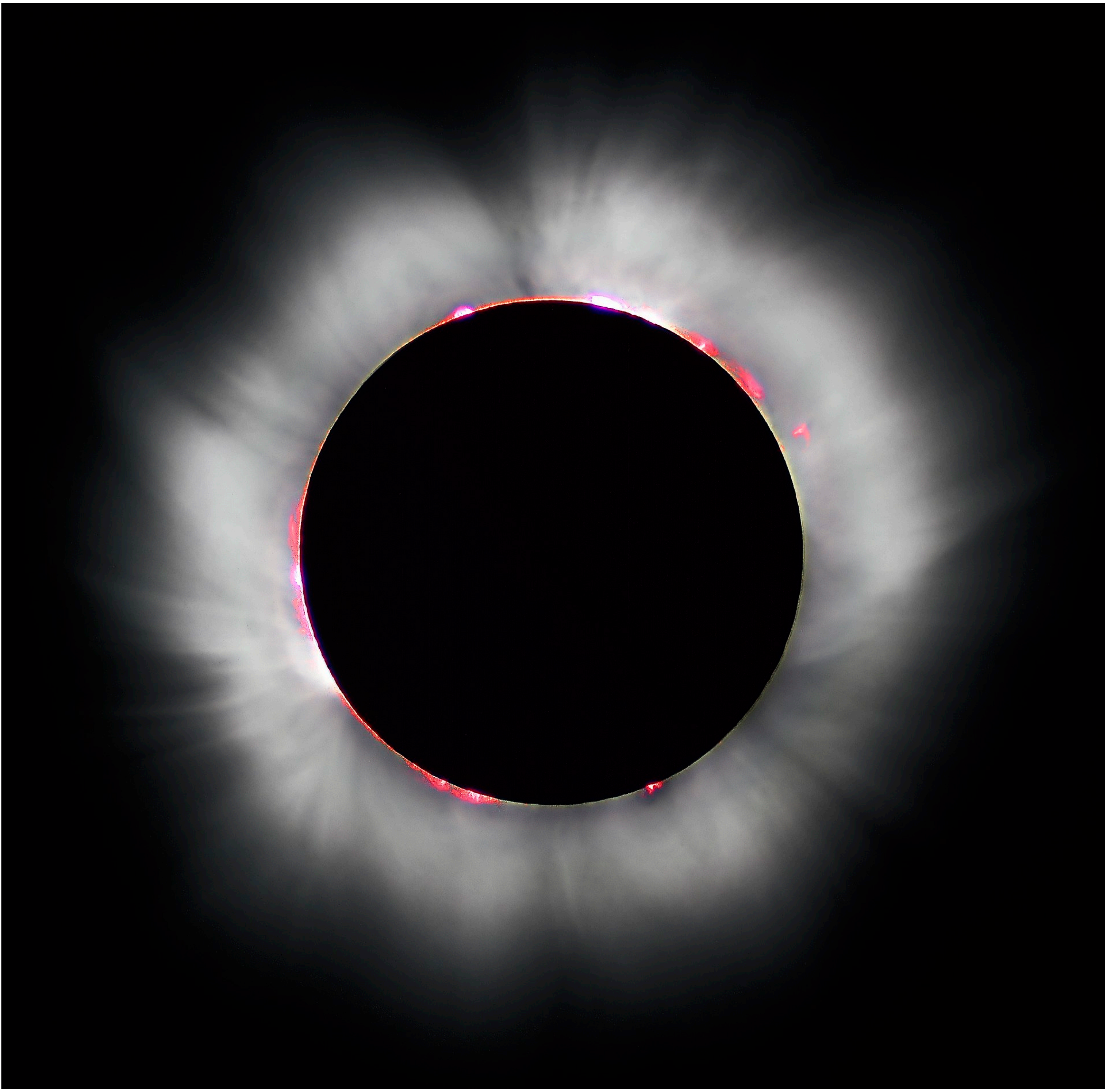

For dark photon DM，the resonant conversion could happen without magnetic Field. We can directly study the resonant conversion process in the solar corona.

Two advantages: closer and larger conversion volume.
Disadvantage: stronger background

During a total solar eclipse, the Sun's corona and prominences are visible to the naked eye.

Generalisation to dark photon DM case

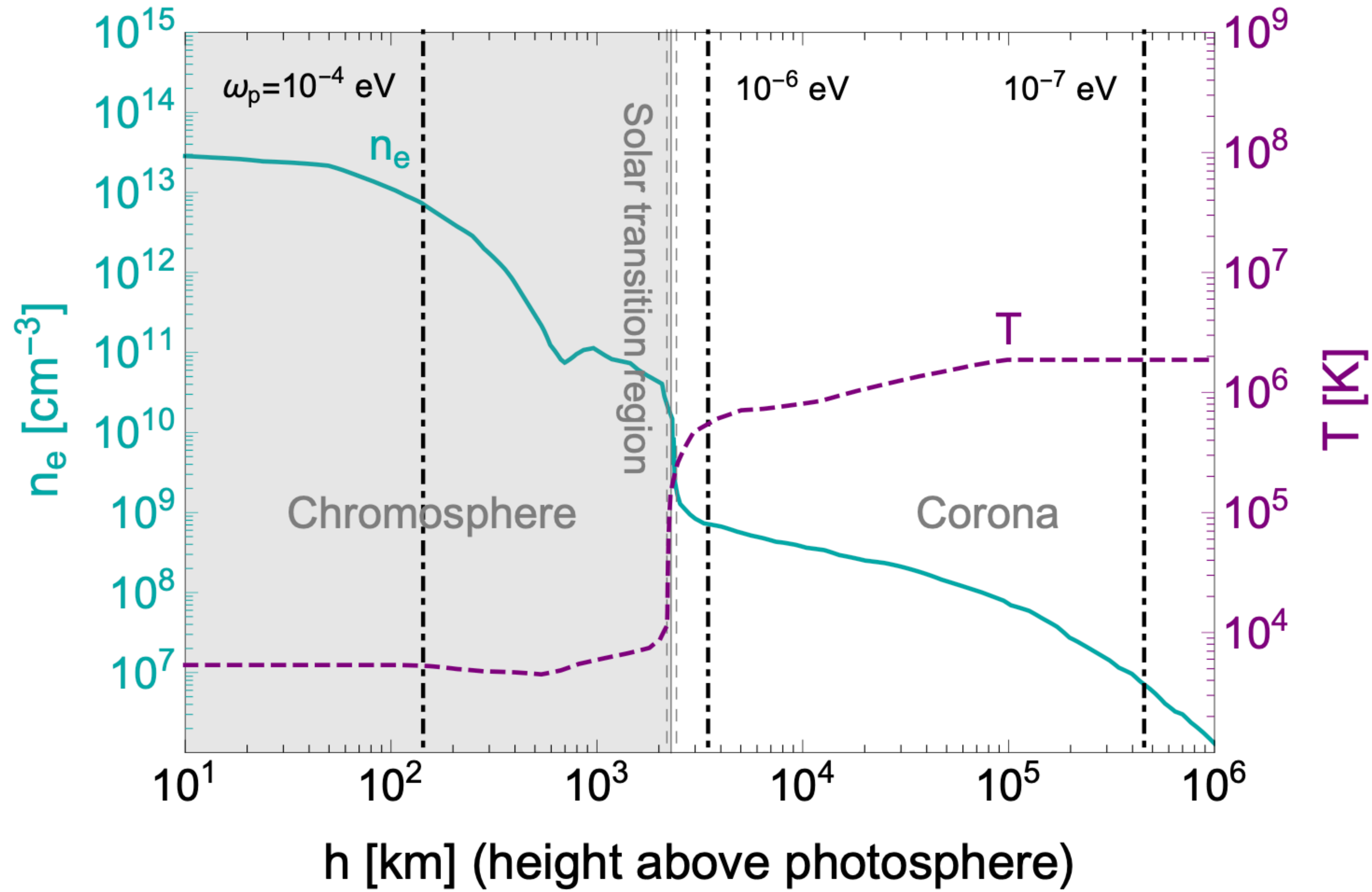

Resonant production

Radio-frequency Dark Photon Dark Matter across the Sun, **Haipeng An, FPH, Jia Liu, Wei Xue arXiv:2010.15836 Phy. Rev. Lett.126, 181102 (2021)**

$$P_{A'\to\gamma}(v_r) = \frac{1}{3}\int \frac{\mathrm{d}t}{2\omega}\frac{\mathrm{d}^3 p}{(2\pi)^3 2\omega}(2\pi)^4\delta^4\left(p^\mu_{A'} - p^\mu_\gamma\right)\sum_{\text{pol}}|\mathcal{M}|^2$$

$$= \frac{2}{3}\times\pi\,\epsilon^2\, m_{A'}\, v_r^{-1}\left|\frac{\partial\ln\omega_p^2(r)}{\partial r}\right|^{-1}_{\omega_p(r)=m_{A'}}, \quad (3)$$

$$\frac{d\mathcal{P}}{d\Omega} \approx 2\times\frac{1}{4\pi}\rho_{\rm DM}\, v_0\int_0^b \mathrm{d}z\, 2\pi z\, P_{A'\to\gamma}(v_r)$$

$$= P_{A'\to\gamma}(v_0)\,\rho_{\rm DM}\, v(r_c)\; r_c^2\,,$$

Propagation effects

It turns out that the dominant absorption process is the inverse bremsstrahlung process.

$$\Gamma_{\rm inv} \approx \frac{8\pi n_e n_N \alpha^3}{3\omega^3 m_e^2}\left(\frac{2\pi m_e}{T}\right)^{1/2}\log\left(\frac{2T^2}{\omega_p^2}\right)\left(1-e^{-\omega/T}\right)$$

$$\Gamma_{\rm Com} = \frac{8\pi\alpha^2}{3m_e^2}n_e.$$

$$P_s \equiv e^{-\int \Gamma_{\rm att} dt} \simeq \exp\left(-\int_{r_c}^{r_{\rm max}} \Gamma_{\rm att} dr/v_r\right)$$

Sensitivity of radio telescope

The minimum detectable flux density of a radio telescope is

$$S_{\rm min} = \frac{\rm SEFD}{\eta_s \sqrt{n_{\rm pol}\, \mathcal{B}\, t_{\rm obs}}}$$

$$\mathrm{SEFD} = 2k_B \frac{T_{\rm sys} + T_{\odot}^{\rm nos}}{A_{\rm eff}}$$

Name	f [MHz]	$B_{\rm res}$ [kHz]	$\langle T_{\rm sys}\rangle$ [K]	$\langle A_{\rm eff}\rangle$ [m^2]
SKA1-Low	(50, 350)	1	680	2.2×10^5
SKA1-Mid B1	(350, 1050)	3.9	28	2.7×10^4
SKA1-Mid B2	(950, 1760)	3.9	20	3.5×10^4
LOFAR	(10, 80)	195	28,110	1,830
LOFAR	(120, 240)	195	1,770	1,530

The sensitivity reach

Haipeng An, FPH, Jia Liu, Wei Xue, Phy. Rev. Lett.126, 181102 (2021)

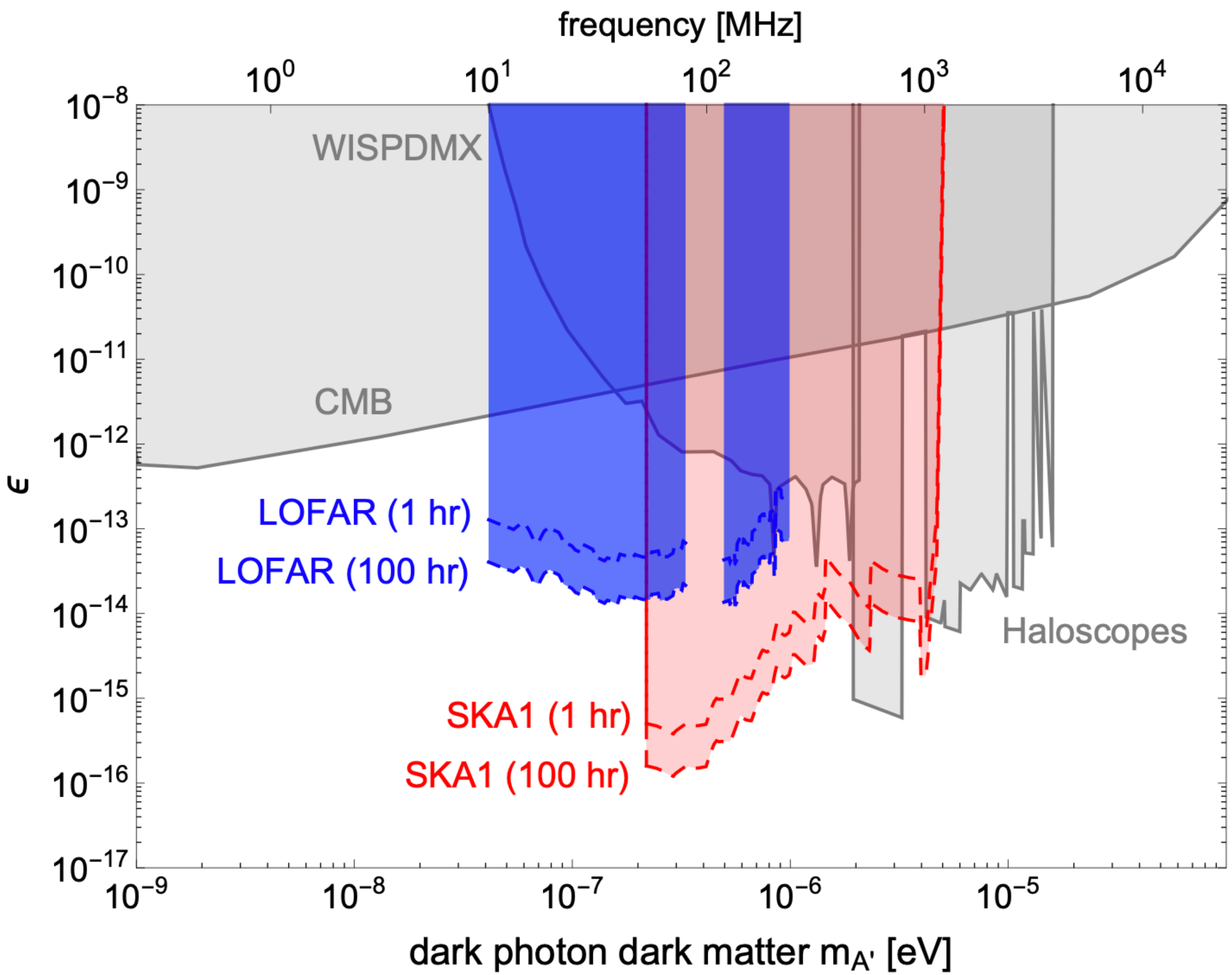

超轻轴子暗物质的双星引力波探测

超轻的暗物质的存在，在双星系统的各个阶段都可能对产生的引力波信号产生可观测的影响

Inspiral：dynamical friction, superradiance, dipole radiation…

Merge: modify the equation of state of the quark/gluon plasma in neutron state, tidal effects

因此，可以通过引力波信号的精确观测来探索超轻暗物质

Imprints of ultralight axions on the gravitational wave signals of neutron star-black hole binary，Ning Xie, FPH, arXiv:2207.11145 and work in progress

超轻轴子暗物质的引力波信号

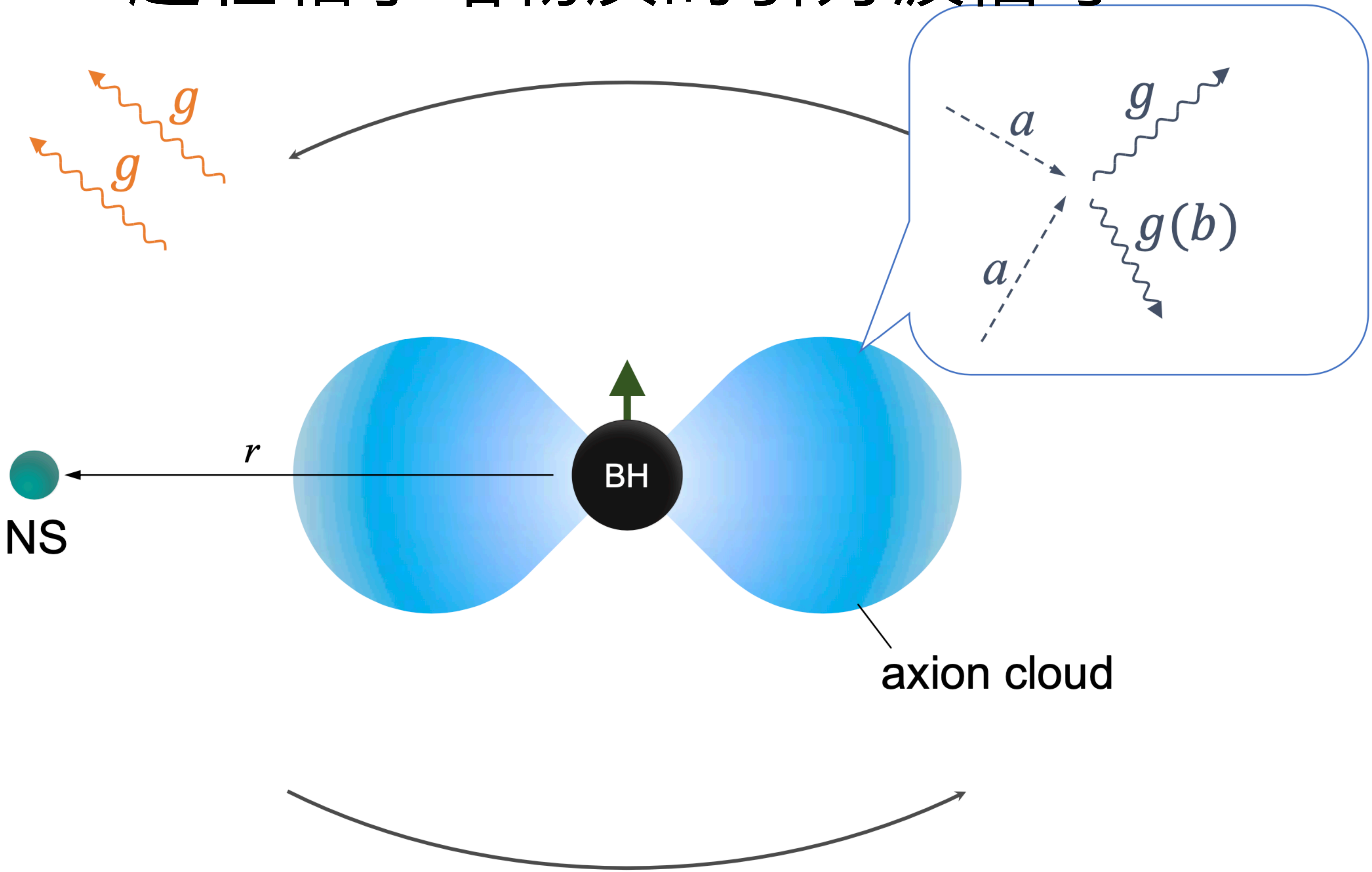

Imprints of ultralight axions on the gravitational wave signals of neutron star-black hole binary，Ning Xie, FPH, arXiv:2207.11145 and work in progress

超轻轴子暗物质的引力波信号

Superradiance: the wave analog of the Penrose process.

Penrose '71
Zel'dovich '72
Starobinsky '73

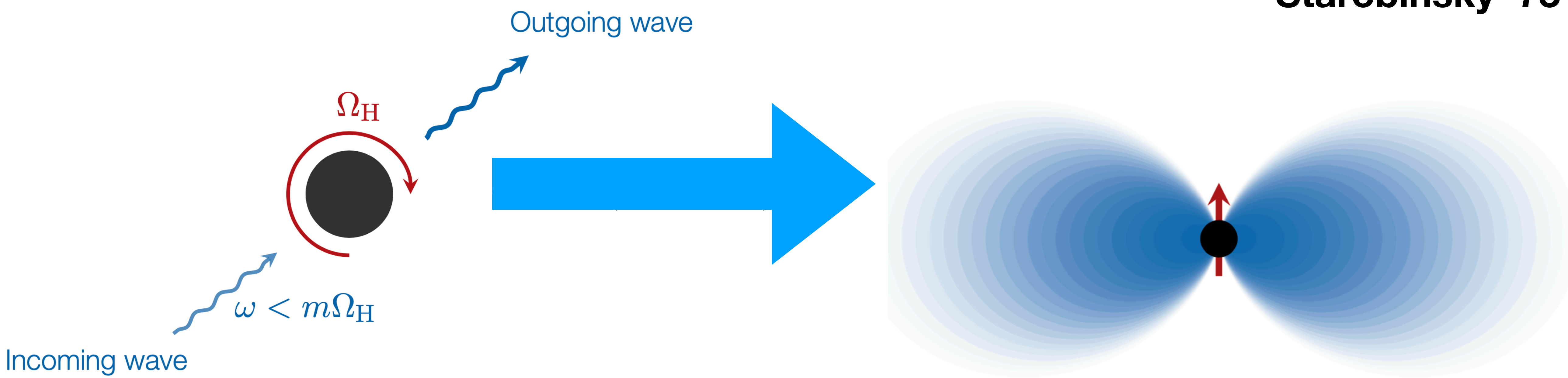

Ultralight axion can form bound states around rotating BH

This resembles the hydrogen atom and is called gravitational atom.

$$\alpha = M_{BH} m_a < 1$$

Credit: Baumann

Saturation time scale of axion cloud growth

$$\tau_{\rm SR} = 1 \text{ day} \left(\frac{M_{\rm BH}}{100 \text{ M}_\odot}\right)\left(\frac{0.2}{\alpha}\right)^9\left(\frac{0.9}{\chi}\right)$$

Annihilation rate for one pair of axions

$$\Gamma_a \simeq \frac{1}{320}\alpha^{12} m_a^3$$

Mass depletion rate of gravitational atom

$$\frac{\tilde{\mathcal{P}}}{M_{\rm BH}} \approx 10^{-6} \text{ yr}^{-1}\left(\frac{m_a}{10^{-12} \text{ eV}}\right) \text{ (for } \alpha = 0.2)$$

超轻轴子暗物质的引力波信号

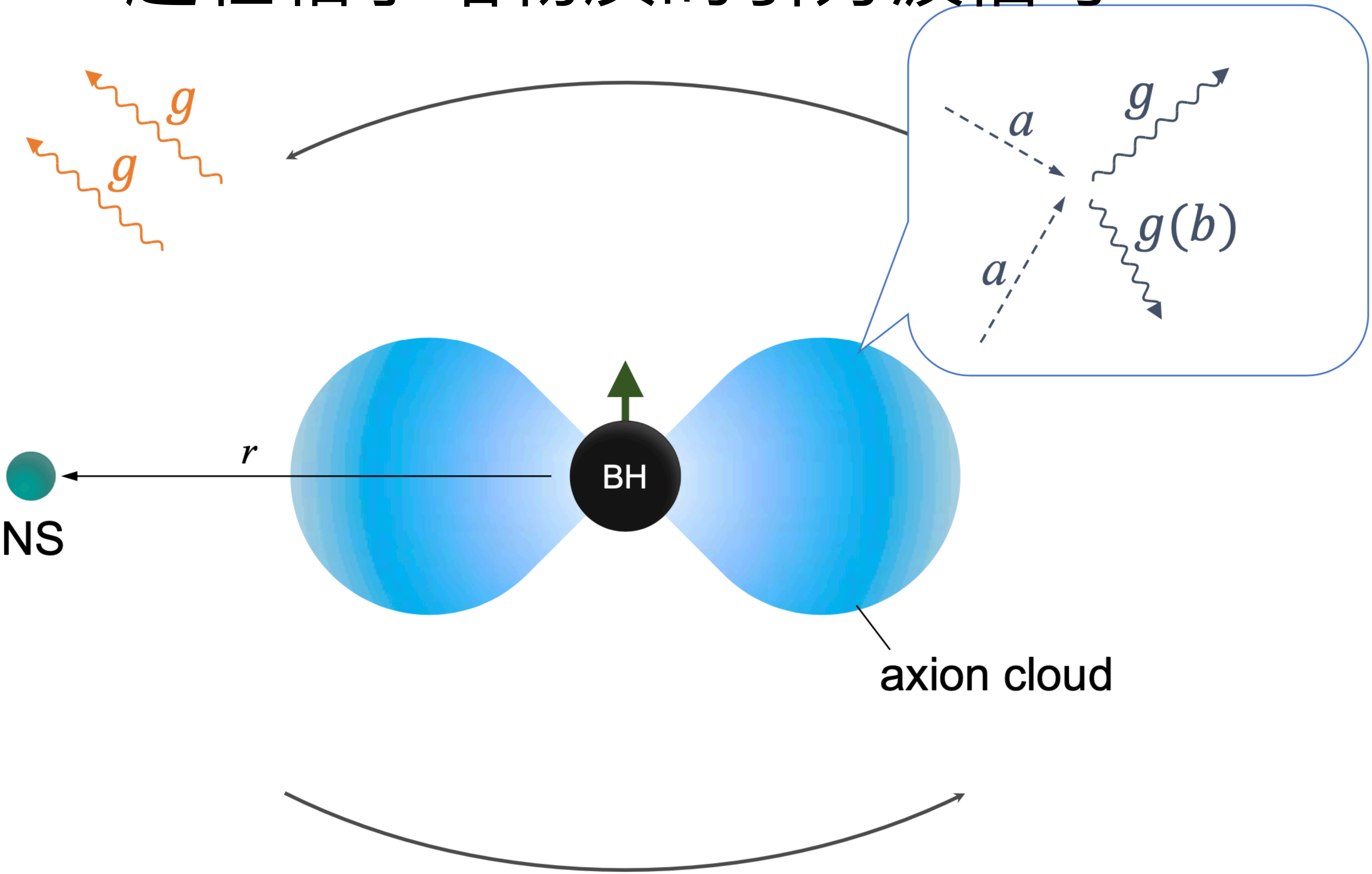

Imprints of ultralight axions on the gravitational wave signals of neutron star-black hole binary，**Ning Xie, FPH**, arXiv:2207.11145 and work in progress

超轻轴子暗物质的引力波信号

Imprints of ultralight axions on the gravitational wave signals of neutron star-black hole binary **Ning Xie, FPH**, arXiv:2207.11145

Without ultralight axions

$$-\frac{\mathrm{d}E_0}{\mathrm{d}t} = \mathcal{P}_{\mathrm{GW}} \qquad \mathcal{P}_{\mathrm{GW}} = \frac{32}{5}\mu^2 r^4 \omega^6$$

$$\omega = \pi f = \sqrt{\frac{M_{\mathrm{BH}} + m_{\mathrm{NS}}}{r^3}}$$

With ultralight axions

$$-\frac{dE}{dt} = (\mathcal{P}_{\mathrm{GW}} + \mathcal{P}_{\mathrm{DC}} + \mathcal{P}_{\mathrm{DF}} + \mathcal{P}_{\mathrm{DR}})$$

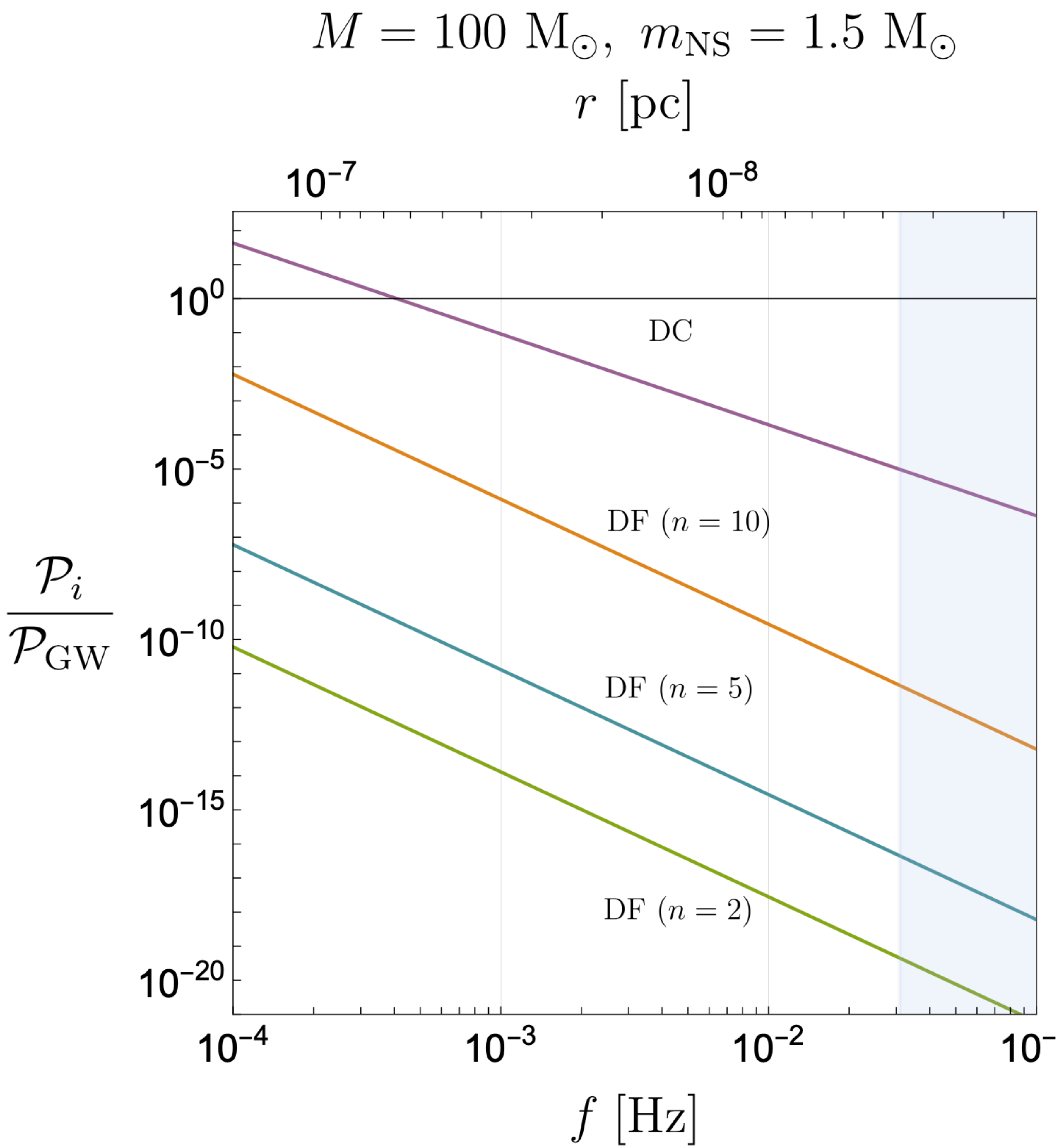

$M = 100\ \mathrm{M}_\odot,\ m_{\rm NS} = 1.5\ \mathrm{M}_\odot$
r [pc]
10^{-7}
10^{-8}
10^{0}
10^{-5}
10^{-10}
10^{-15}
10^{-20}
$\frac{\mathcal{P}_i}{\mathcal{P}_{\rm GW}}$
DC
DF ($n = 10$)
DF ($n = 5$)
DF ($n = 2$)
10^{-4}
10^{-3}
10^{-2}
10^{-1}
f [Hz]

超轻轴子暗物质的引力波信号

Imprints of ultralight axions on the gravitational wave signals of neutron star-black hole binary

Ning Xie, FPH, arXiv:2207.11145

$$\frac{\mathrm{d}r}{\mathrm{d}t} = \left(-\frac{M m_{\rm NS}}{2r^2}\right)^{-1} (\mathcal{P}_{\rm GW} + \mathcal{P}_{\rm DC} + \mathcal{P}_{\rm DF} + \mathcal{P}_{\rm DR})$$

$$\Delta\phi \sim 15\pi \left(\frac{m_a}{10^{-12}\ \mathrm{eV}}\right) \left(\frac{f_T}{10^{-2}\ \mathrm{Hz}}\right) \left(\frac{T}{5\ \mathrm{yrs}}\right)^2$$

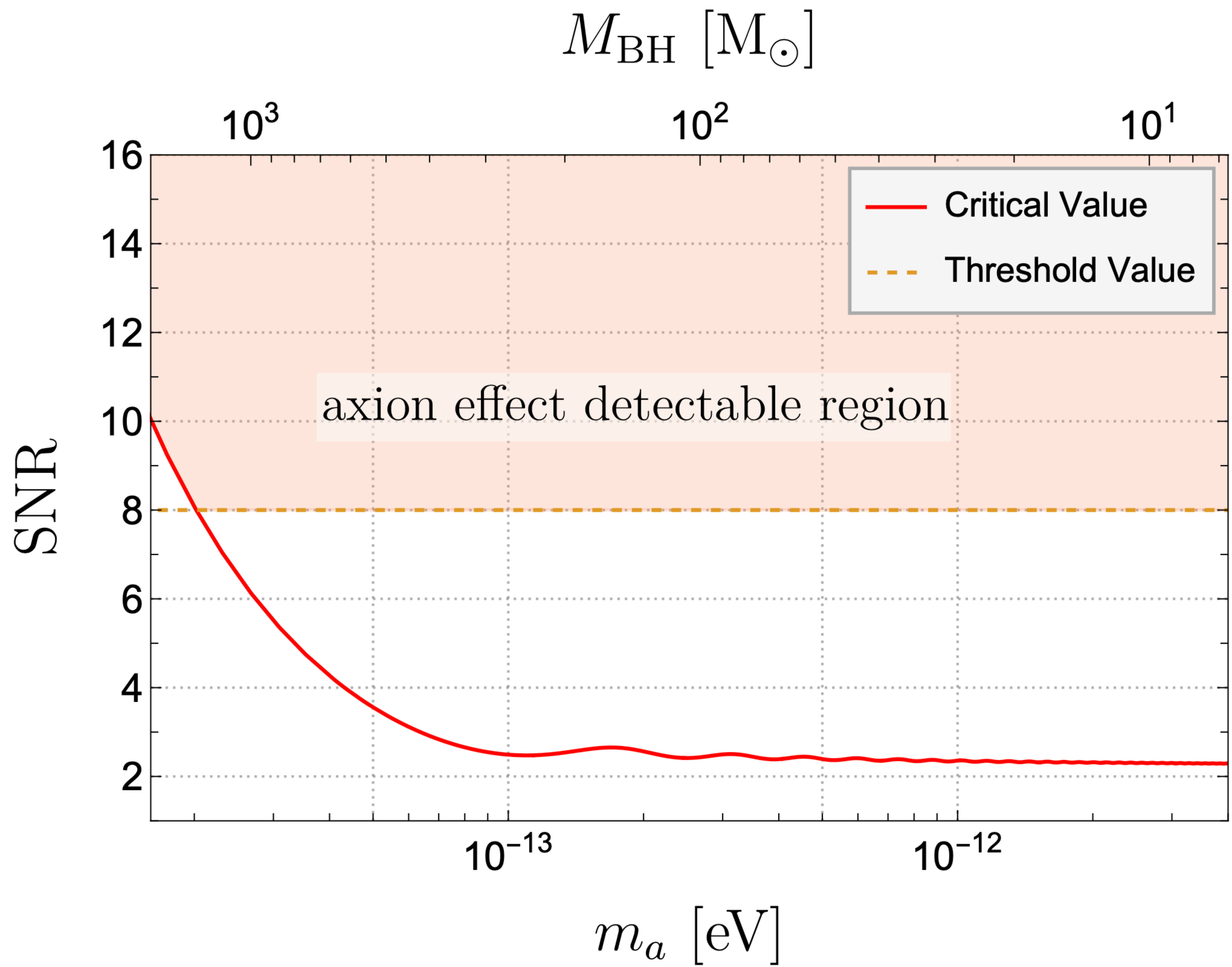

$M_{\rm BH}$ [$\mathrm{M}_\odot$]
10^3
10^2
10^1
16
14
12
10
8
6
4
2
SNR
Critical Value
Threshold Value
axion effect detectable region
10^{-13}
10^{-12}
m_a [eV]

II. 暗物质的相变引力波探测

- ➢The observation of GW by LIGO has initiated a new era of exploring DM by GW.

- ➢ DM can trigger strong first-order phase transition(SFOPT) in the early universe, which can produce detectable GW signals.

- ➢New DM production scenario filtered by the bubbles of SFOPT in the early universe

Hearing the signal of dark sectors with gravitational wave detectors
J.Jaeckel, V. V. Khoze, M. Spannowsky, Phys.Rev. D94 (2016) no.10, 103519

Yan Wang,Chong Sheng Li, and FPH, arXiv:2012.03920
FPH, Eibun Senaha Phys.Rev. D100 (2019) no.3, 03501
FPH PoS ICHEP2018 (2019) 397
FPH, Chong Sheng Li Phys.Rev. D96 (2017) no.9, 095028
FPH, Jiang-Hao Yu Phys.Rev. D98 (2018) no.9, 095022
FPH, Xinmin Zhang, Phys.Lett. B788 (2019) 288-29

早期宇宙的量子遂穿效应

这世上的热闹，源自遂穿

Calculate the finite-temperature effective potential using the thermal field theory: free energy density.

$$V_{\text{eff}}^{(1)}(\bar{\phi}) = \sum_i n_i \Big[\int \frac{\mathrm{d}^D p}{(2\pi)^D} \ln\big(p^2 + m_i^2(\bar{\phi})\big) + J_{\mathrm{B,F}}\Big(\frac{m_i^2(\bar{\phi})}{T^2}\Big) \Big]$$

$$S(T) = \int d^4x \left[\frac{1}{2} \left(\frac{\partial \phi}{\partial x} \right)^2 + V_{\text{eff}}\,(\phi, T) \right]$$

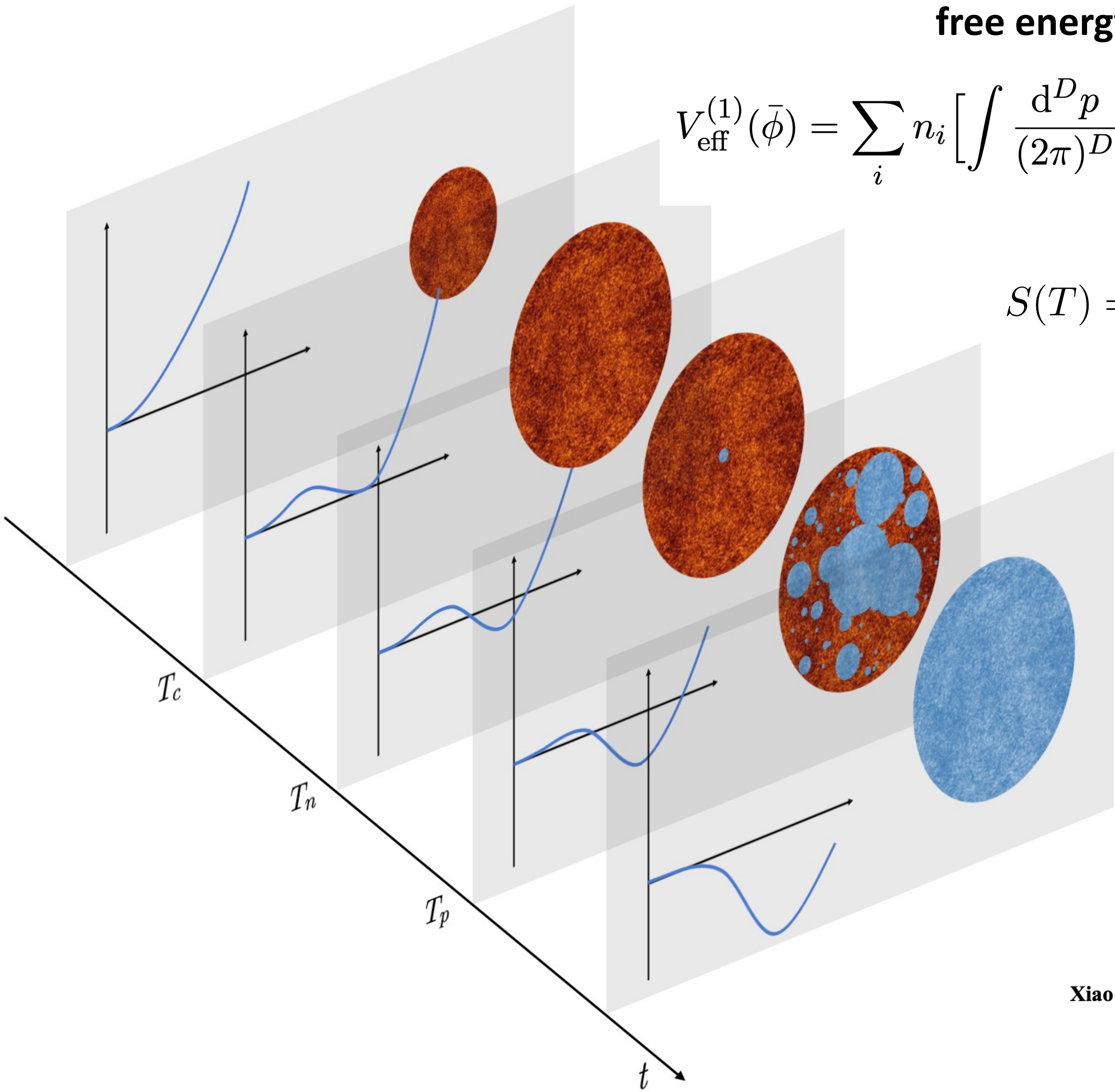

$$\Gamma = \Gamma_0 e^{-S(T)}$$

Xiao Wang, FPH, Xinmin Zhang, JCAP05(2020)045

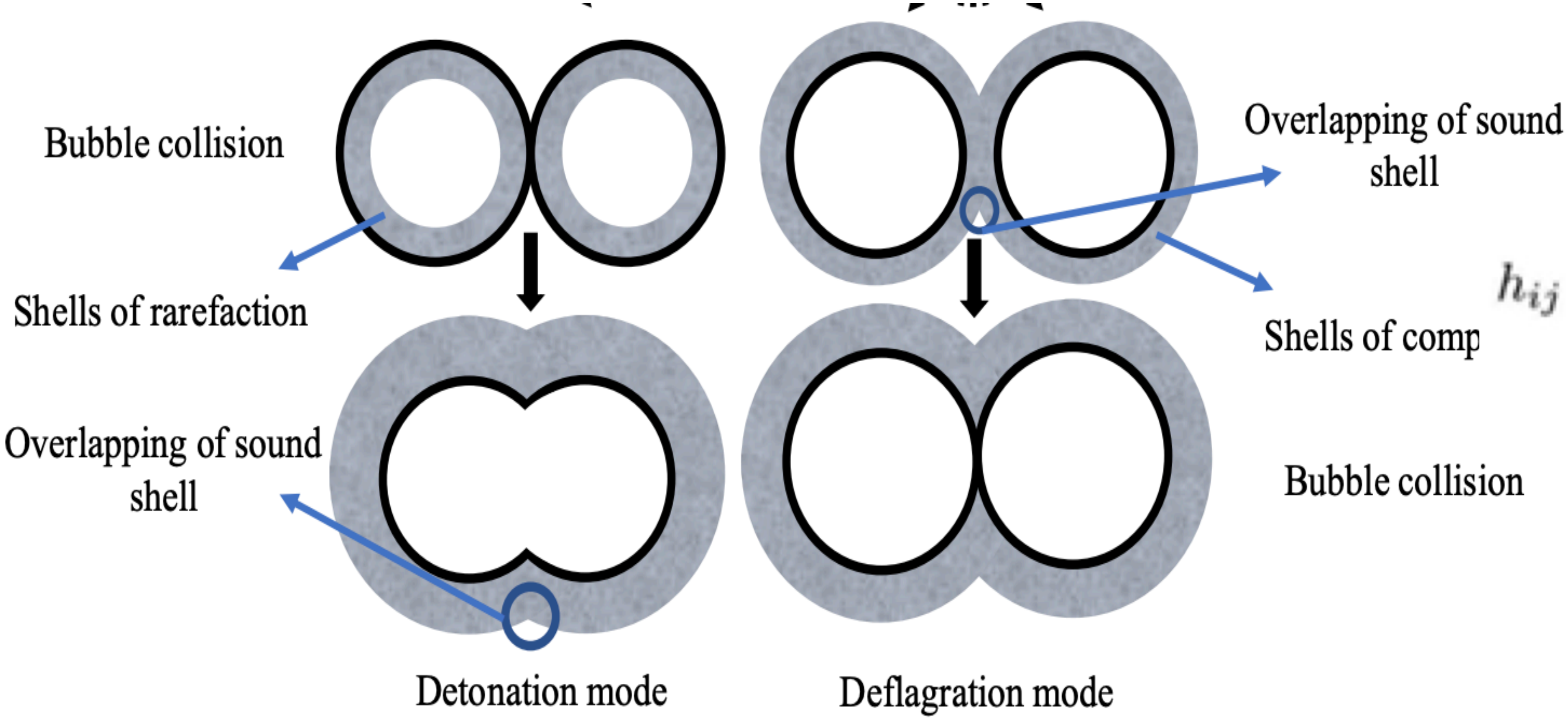

$$h_{ij} \simeq \frac{2G}{c^4 r} \ddot{Q}_{ij}^{TT}(t - r/c)$$

Xiao Wang, FPH, Yongping Li, *Phys.Rev.D* 105 (2022) 10351

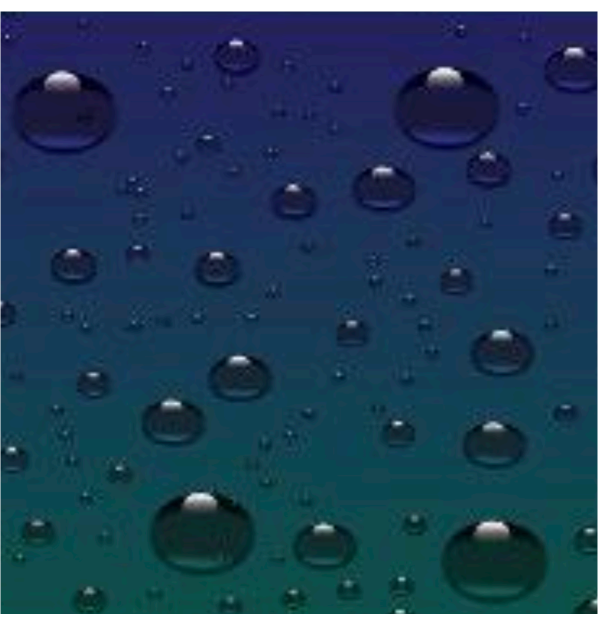

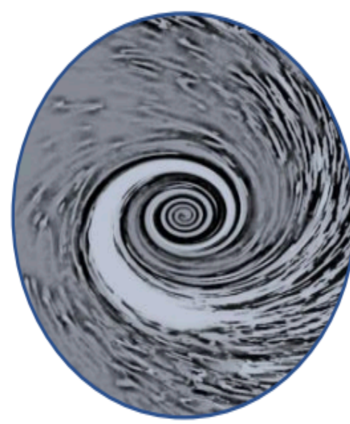

Turbulence

$$R_{\mu\nu} - \frac{1}{2} R\, g_{\mu\nu} + \Lambda\, g_{\mu\nu} = \frac{8\pi G}{c^4} T_{\mu\nu}$$

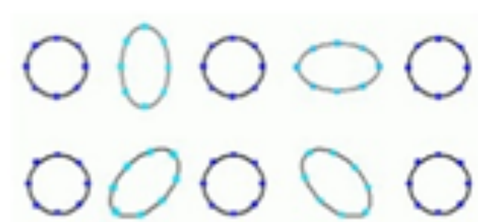

Xiao Wang, FPH, Xinmin Zhang, JCAP05(2020)045

E. Witten, Phys. Rev. D 30, 272 (1984)
C. J. Hogan, Phys. Lett. B 133, 172 (1983);
M. Kamionkowski, A. Kosowsky and M. S. Turner, Phys. Rev. D 49, 2837 (1994))

EW phase transition GW becomes more interesting and realistic after the discovery of Higgs by LHC and GW by LIGO.

$$\ddot{h}_{ij}(\mathbf{x},t) + 3\,H\,\dot{h}_{ij}(\mathbf{x},t) - \frac{\nabla^2}{a^2}\,h_{ij}(\mathbf{x},t) = 16\pi G \boxed{\Pi_{ij}(\mathbf{x},t)}$$

Possible sources of tensor anisotropic stress in the early universe

- Scalar field gradients $\Pi_{ij} \sim [\partial_i\phi\partial_j\phi]^{TT}$ eg. Collisions of bubble walls
- Bulk fluid motion $\Pi_{ij} \sim [\gamma^2(\rho+p)v_iv_j]^{TT}$ eg. Sound waves and turbulence in the fluid
- Gauge fields $\Pi_{ij} \sim [-E_iE_j - B_iB_j]^{TT}$ eg. Primordial magnetic fields (MHD turbulence)
- Second order scalar perturbations, Π_{ij} from a combination of $\partial_i\Psi, \partial_i\Phi$
- ...

arXiv:1801.04268

GW signals from SFOPT

Bubble collisions

$$h^2\Omega_{\rm co}(f) \simeq 1.67\times 10^{-5}\left(\frac{H_* R_*}{(8\pi)^{1/3}}\right)^2 \left(\frac{\kappa_\phi \alpha}{1+\alpha}\right)^2 \left(\frac{100}{g_\star}\right)^{1/3} \frac{0.11 v_b}{0.42+v_b^2}\frac{3.8(f/f_{\rm co})^{2.8}}{1+2.8(f/f_{\rm co})^{3.8}}$$

Turbulence

$$h^2\Omega_{\rm turb}(f) \simeq 1.14\times 10^{-4} H_* R_* \left(\frac{\kappa_{\rm turb}\alpha}{1+\alpha}\right)^{3/2} \left(\frac{100}{g_*}\right)^{1/3} \frac{(f/f_{\rm turb})^3}{(1+f/f_{\rm turb})^{11/3}(1+8\pi f/H_*)}$$

Sound wave

$$h^2\Omega_{\rm sw}(f) \simeq 1.64\times 10^{-6}(H_*\tau_{\rm sw})(H_* R_*) \left(\frac{\kappa_v \alpha}{1+\alpha}\right)^2 \left(\frac{100}{g_*}\right)^{1/3} (f/f_{\rm sw})^3 \left(\frac{7}{4+3(f/f_{\rm sw})^2}\right)^{7/2}$$

E. Witten, Phys. Rev. D 30, 272 (1984)
C. J. Hogan, Phys. Lett. B 133, 172 (1983);
M. Kamionkowski, A. Kosowsky and M. S. Turner, Phys. Rev. D 49, 2837 (1994))Mark Hindmarsh, *et al.*, PRL 112, 041301 (2014); Lots of unlisted papers.

Phase transition dynamics

Precise predictions on the phase transition dynamics and its GW signals

1.Precise finite-temperature effective potential $V_{eff}(\phi, T)$

(1)Daisy resummation: Pawani scheme vs. Arnold scheme

(2)Gauge dependence: see Michael J. Ramsey-Musolf's works

(3)No perturbative calculations: lattice see Michael J. Ramsey-Musolf's works， also Ligong's recent work

and dim-reduction method: by D. Weir, Michael J. Ramsey-Musolf et.al

2. Reliable calculations of bubble wall velocity v_b

S. Hoche, J. Kozaczuk, A. J. Long, J. Turner and Y. Wang， arXiv:2007.10343，
Avi Friedlander, Ian Banta, James M. Cline, David Tucker-Smith， arXiv:2009.14295v2
Xiao Wang, FPH, Xinmin Zhang,arXiv:2011.12903

3. Energy budget during phase transition

F. Giese, T. Konstandin, K. Schmitz and J. van de Vis,arXiv:2010.09744
Xiao Wang,**FPH** and Xinmin Zhang, arXiv:2010.13770 κ
物理讨论见晁伟老师的报告

Phase transition Dynamics

Classify the SFOPT into four cases:

- **Slight supercooling**: $\alpha_p < 0.1$ GW is too weak to be detected by LISA, might be within the sensitivity of BBO and ultimate-DECIGO.
- **Mild supercooling:** $0.1 < \alpha_p < 0.5$ the GW could be detected by LISA, TianQin, Taiji, BBO, DECIGO.
- **Strong supercooling:** $0.5 < \alpha_p < 1$
- **Ultra supercooling:** $\alpha_p > 1$

Xiao Wang, FPH, Xinmin Zhang, JCAP05(2020)045

- **The observation of GW by LIGO has initiated a new era of exploring DM by GW.**
- **DM can trigger a SFOPT in the early universe, which can leads to detectable GW signals.**

Hearing the signal of dark sectors with gravitational wave detectors
J.Jaeckel, V. V. Khoze, M. Spannowsky, Phys.Rev. D94 (2016) no.10, 103519
Zhaofeng Kang,et.al. arXiv:2101.03795
Zhaofeng Kang, et. al. arXiv:2003.02465
Yan Wang, Chong Sheng Li, and **FPH**, arXiv:2012.03920
FPH, Eibun Senaha Phys.Rev. D100 (2019) no.3, 03501
FPH PoS ICHEP2018 (2019) 397
FPH, Chong Sheng Li, Phys.Rev. D96 (2017) no.9, 095028
FPH, Jiang-Hao Yu, Phys.Rev. D98 (2018) no.9, 095022
FPH, Xinmin Zhang, Phys.Lett. B788 (2019) 288-29

相变引力波探测暗物质直接探测盲区

Inert Doublet Models

$$V_0 = M_D^2 D^\dagger D + \lambda_D (D^\dagger D)^2 + \lambda_3 \Phi^\dagger \Phi D^\dagger D + \lambda_4 |\Phi^\dagger D|^2 + (\lambda_5/2)[(\Phi^\dagger D)^2 + h.c.],$$

mixed singlet-doublet model

$$V_0 = \frac{1}{2} M_S^2 S^2 + M_D^2 H_2^\dagger H_2 + \frac{1}{2}\lambda_S S^2 |\Phi|^2 + \lambda_3 \Phi^\dagger \Phi H_2^\dagger H_2 + \lambda_4 |\Phi^\dagger H_2|^2 + \frac{\lambda_5}{2}[(\Phi^\dagger H_2)^2 + \mathrm{H.c.}] + A[S\Phi H_2^\dagger + \mathrm{H.c.}].$$

mixed singlet-triplet model

$$V_0 = \frac{1}{2} M_S^2 S^2 + M_\Sigma^2 \mathrm{Tr}(H_3^2) + \kappa_\Sigma \Phi^\dagger \Phi \mathrm{Tr}(H_3^2) + \frac{\kappa}{2} |\Phi|^2 S^2 + \xi S \Phi^\dagger H_3 \Phi.$$

provide natural DM candidate

produce SFOPT and phase transition GW

FPH, Jiang-Hao Yu, Phys.Rev. D98 (2018) no.9, 095022
Yan Wang, Chong Sheng Li, and **FPH**, *Phys.Rev.D* 104 (2021) 5, 053004;

Inert Doublet DM Models

The tree-level potential to describe the inert doublet DM model is given by

$$V_0 = M_D^2 D^\dagger D + \lambda_D (D^\dagger D)^2 + \lambda_3 \Phi^\dagger \Phi D^\dagger D + \lambda_4 |\Phi^\dagger D|^2 + (\lambda_5/2)[(\Phi^\dagger D)^2 + h.c.],$$

provide natural DM candidate

provide SFOPT and phase transition GW

FPH, Jiang-hao Yu, Phy. Rev. D 98, 095022 (2018)
Yan Wang, Chong Sheng Li, FPH, arXiv: 2012.03920

One example：

The mixed singlet-doublet DM model

The tree-level potential to describe the mixed singlet-doublet DM model is given by

$$V_0 = \frac{1}{2}M_S^2 S^2 + M_D^2 H_2^\dagger H_2 + \frac{1}{2}\lambda_S S^2 |\Phi|^2 + \lambda_3 \Phi^\dagger \Phi H_2^\dagger H_2 + \lambda_4 |\Phi^\dagger H_2|^2 + \frac{\lambda_5}{2}[(\Phi^\dagger H_2)^2 + \text{H.c.}] + A[S\Phi H_2^\dagger + \text{H.c.}].$$

provide natural DM candidate

produce SFOPT and phase transition GW

FPH, Jiang-hao Yu, Phy. Rev. D 98, 095022 (2018)

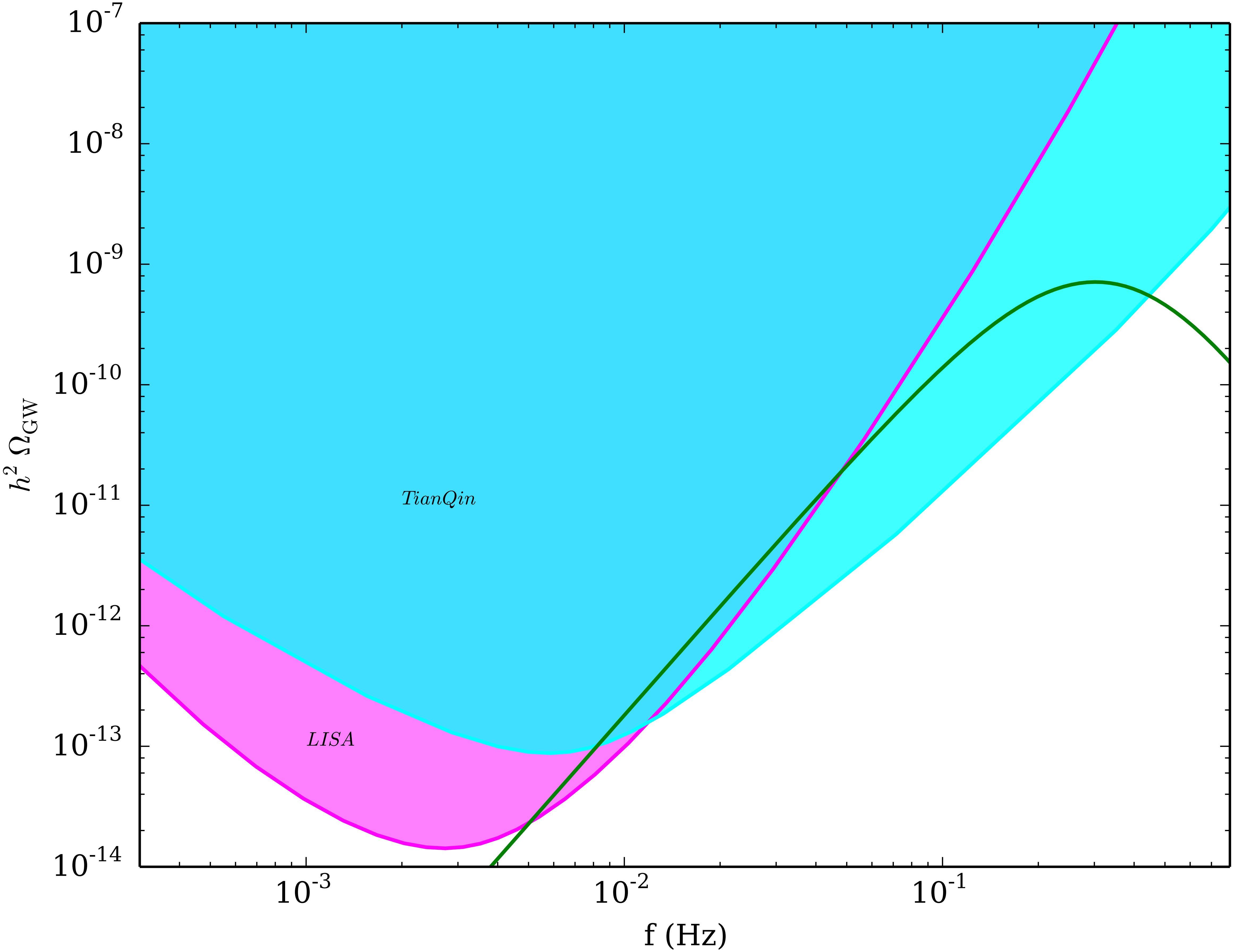

10^{-7}
10^{-8}
10^{-9}
10^{-10}
10^{-11}
10^{-12}
10^{-13}
10^{-14}
$h^2\,\Omega_{\rm GW}$
TianQin
LISA
10^{-3}
10^{-2}
10^{-1}
f (Hz)

Heavy DM formed by SFOPT

Renaissance of quark nugget DM by Witten

The cosmic phase transition with Q-balls production can explain baryogenesis and DM simultaneously, where constraints on DM mass and reverse dilution are significantly relaxed. We study how to probe this scenario by GW signals and collider signals at QCD NLO.

FPH, Chong Sheng Li, Phys. Rev. D96 (2017) no.9, 095028

SFOPT naturally correlates DM, baryogenesis, particle collider and GW signals.

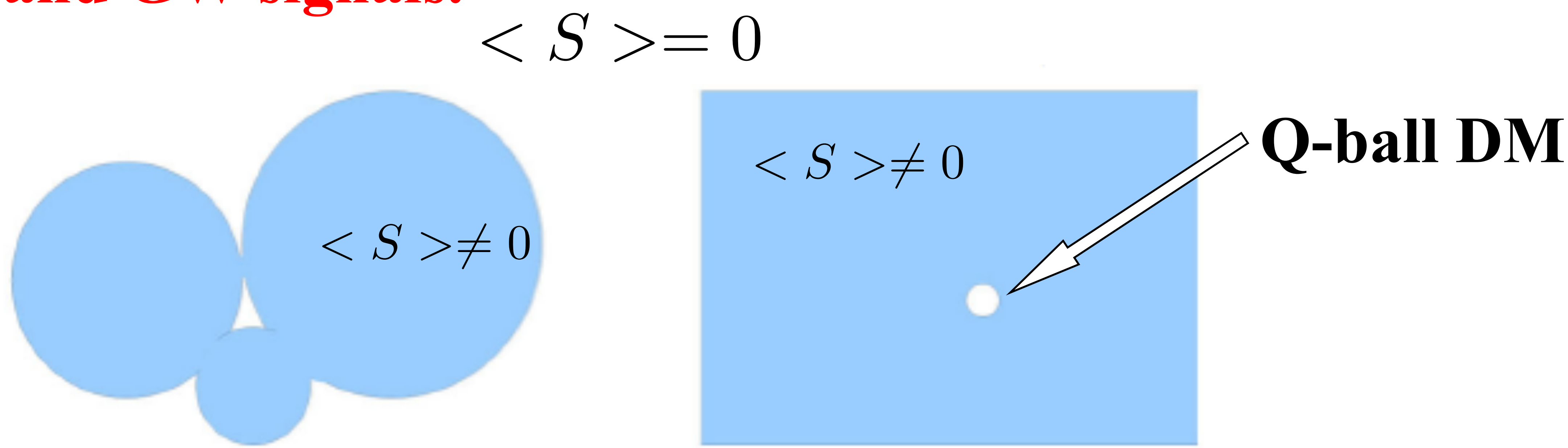

And with the bubble expansion, the symmetric phase eventually shrinks to very small size objects and become the so-called Q-balls as DM candidates.

$$
\begin{aligned}
\mathcal{L} = & \frac{1}{2}(\partial_\mu S)^2 - U(S) + (\partial_\mu \chi)^*(\partial_\mu \chi) - k_1^2 S^2 \chi^* \chi \\
& - \sum_i \frac{h_i^2}{2} S^2 \phi_i^2 + \sum_i \frac{1}{2}(\partial_\mu \phi_i)^2 \\
& - \sum_{a=1,2} \frac{\lambda_a^{ijk}}{\Lambda^2} \bar{X}_a P_R D_i \bar{U}_j^C P_R D_k + \frac{\zeta_a}{\Lambda} \bar{X}_a Y^C \chi \chi^* \\
& + \mathrm{H.c.}
\end{aligned}
$$

Final conditions to produce the observed baryon asymmetry and DM density: **FPH**, C.S. Li, **Phys.Rev. D96 (2017) no.9, 09502**

$$\rho_{\mathrm{DM}}^4 v_b^{3/4} = 73.5(2\eta_B s_0)^3 \lambda_S \sigma^4 \Gamma^{3/4}$$

TABLE I. The benchmark sets after considering the combined constraints for producing the observed DM density and BAU with $v_b = 0.3$.

Benchmark sets	λ_S	e	c	T_c [TeV]	$\frac{\sigma}{T_C}$
I	0.008	0.754	1	15.9	5
II	0.0016	0.151	1	6.6	5

Extension work for the gauged Q-balls is working in progress with P. Ko and Xiao Wang

The predicted GW spectrum with $v_b = 0.3$. Figure(a), (b), (c) represents the GW spectrum from bubble collision, sound waves and turbulence, respectively, which may be detected by future LIGO-like experiments, Einstein telescope or cosmic explorer.

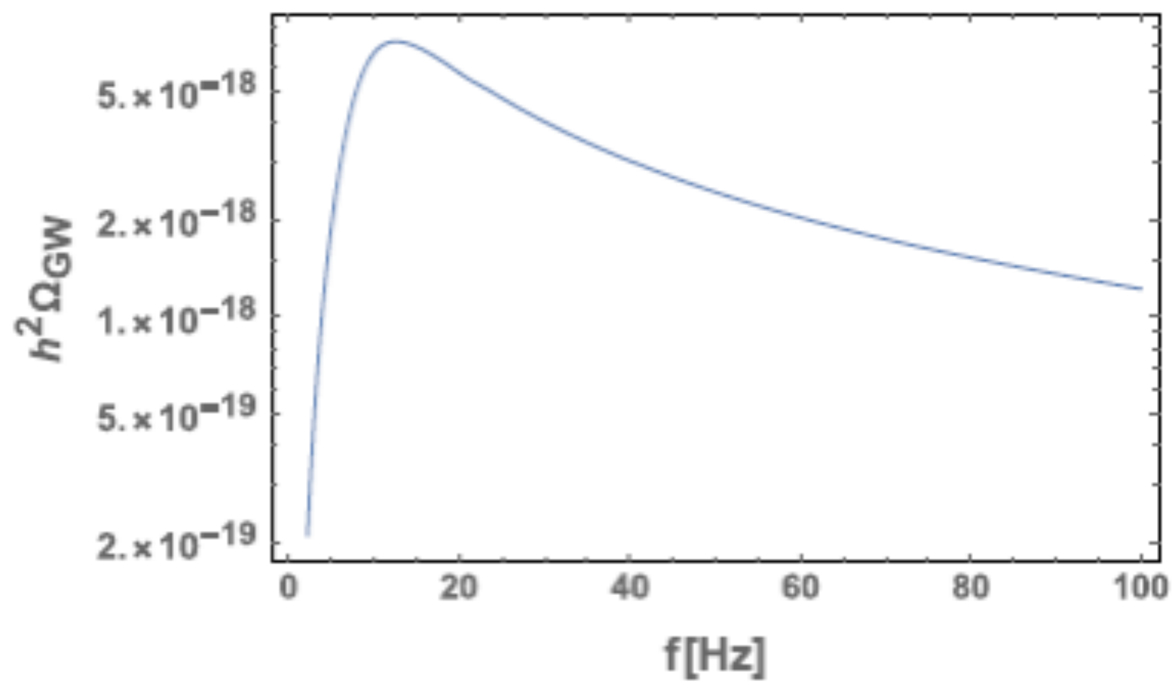

(a)

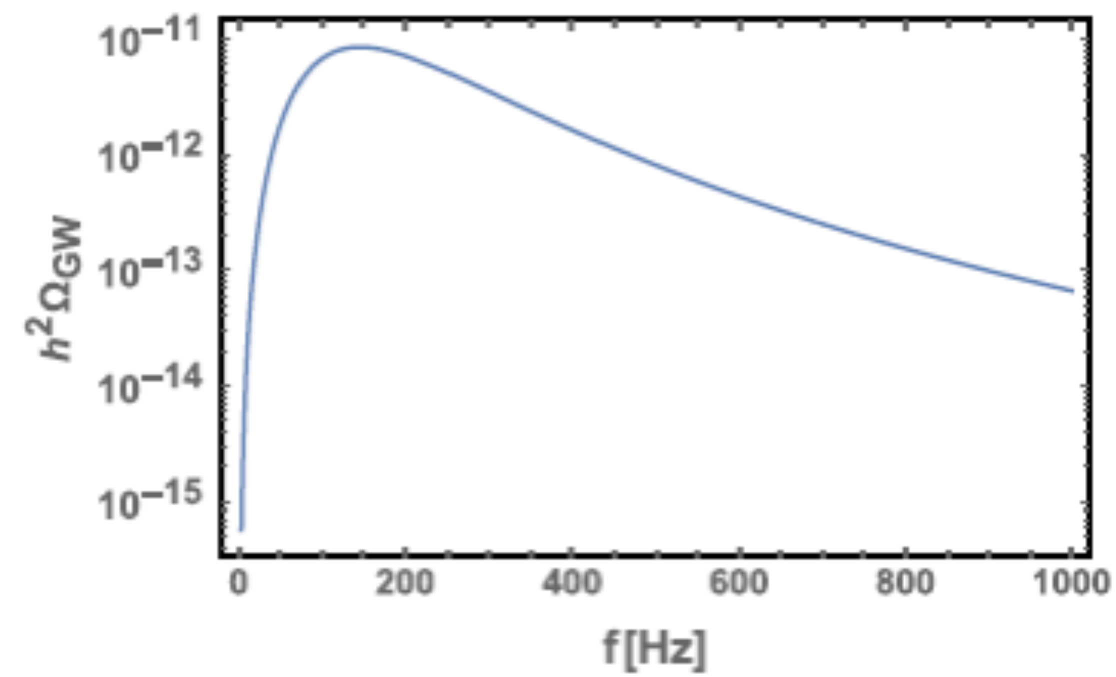

(b)

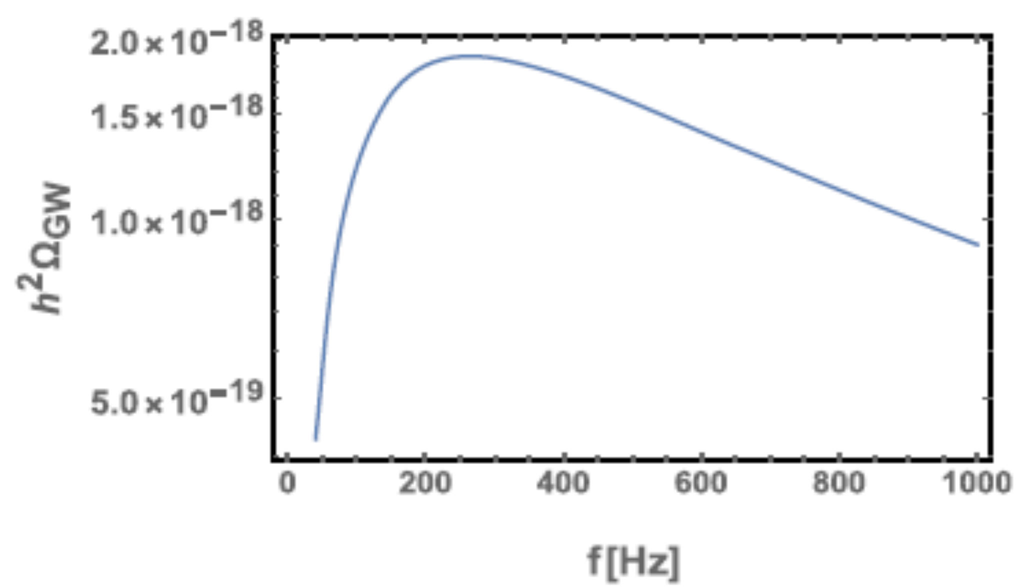

(c)

Collider phenomenology

There are many types of combinations for the up-type quark and down-type quark, which result in abundant collider phenomenology at the LHC.

The dominant decay channel behaves as the missing energy in the detector. So the interactions can be explored by performing mono-jet and mono-top analysis at the LHC.

Because the LHC is a proton-proton collider with high precision, the QCD NLO predictions for these processes are necessary in order to obtain reliable results.

QCD NLO prediction at the LHC

We perform QCD the next-leading-order (NLO) predictions for these two cases and discuss the discovery potential at the LHC.

The Key point for QCD NLO calculation is Infrared divergence

Origin of singular contributions: soft and collinear emission

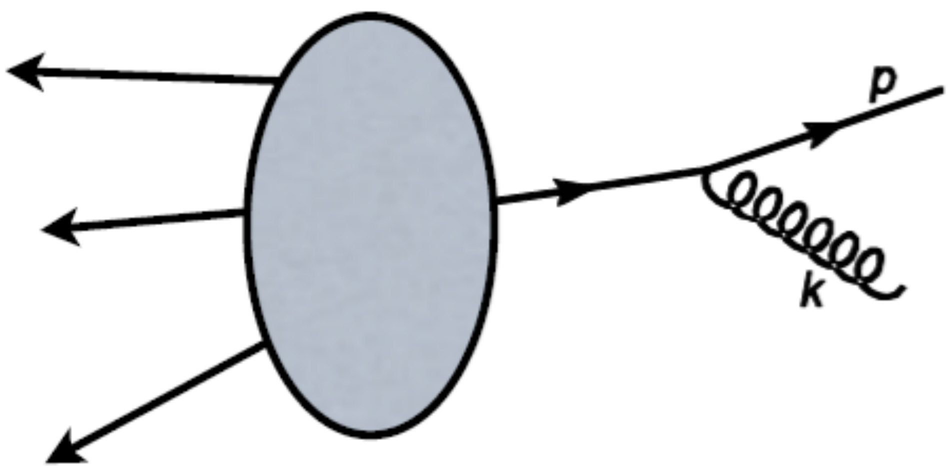

$$\frac{1}{(p+k)^2} = \frac{1}{2\,p\cdot k} = \frac{1}{2E_qE_g(1-\cos\theta_{qg})}$$

soft collinear

Tricks for QCD NLO calculations:
Two cutoff phase space slicing method (δs,δc)
or dipole subtraction

Mono-jet analysis at QCD NLO

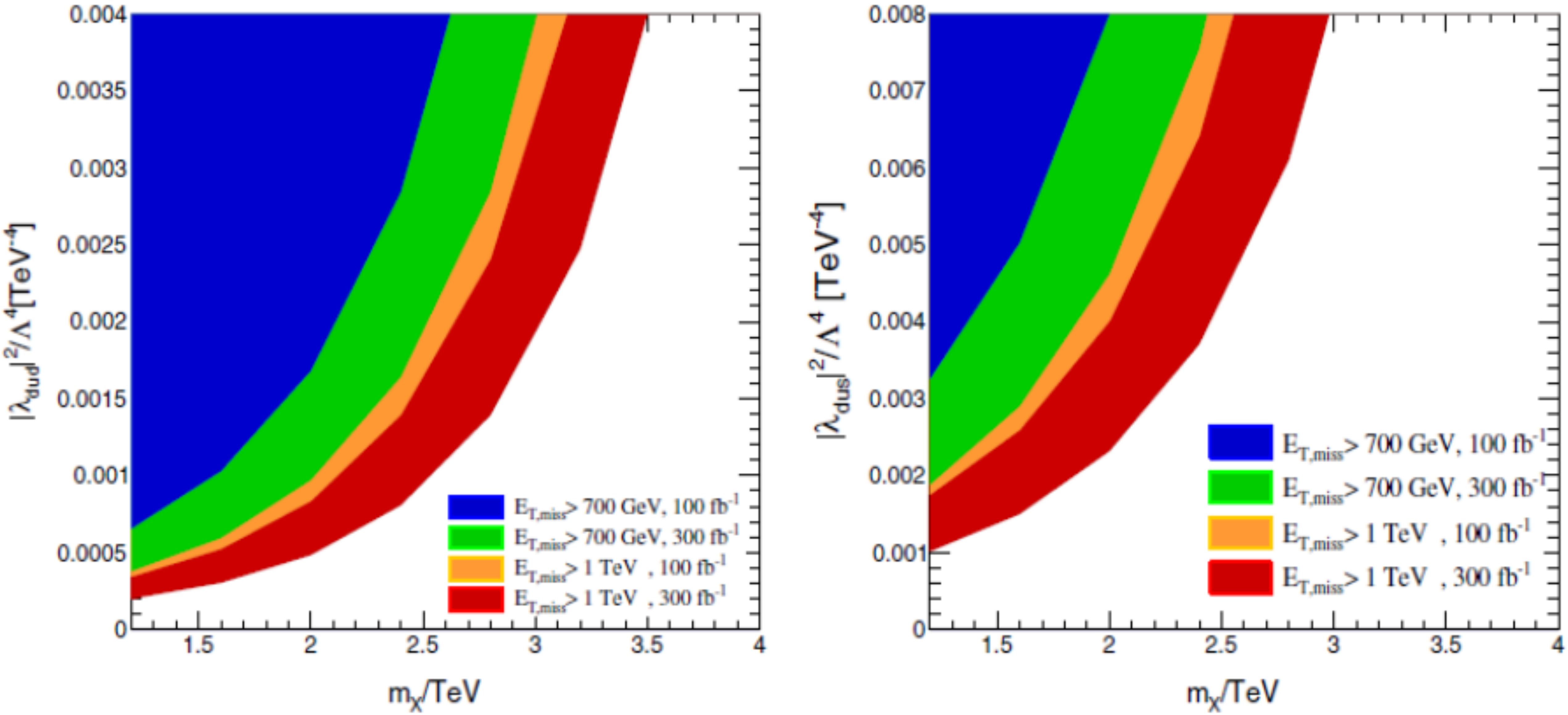

Constraints on coupling λ_{ijk} and mass m_X by monojet measurements at the 13 TeV LHC.

Mono-top analysis at QCD NLO

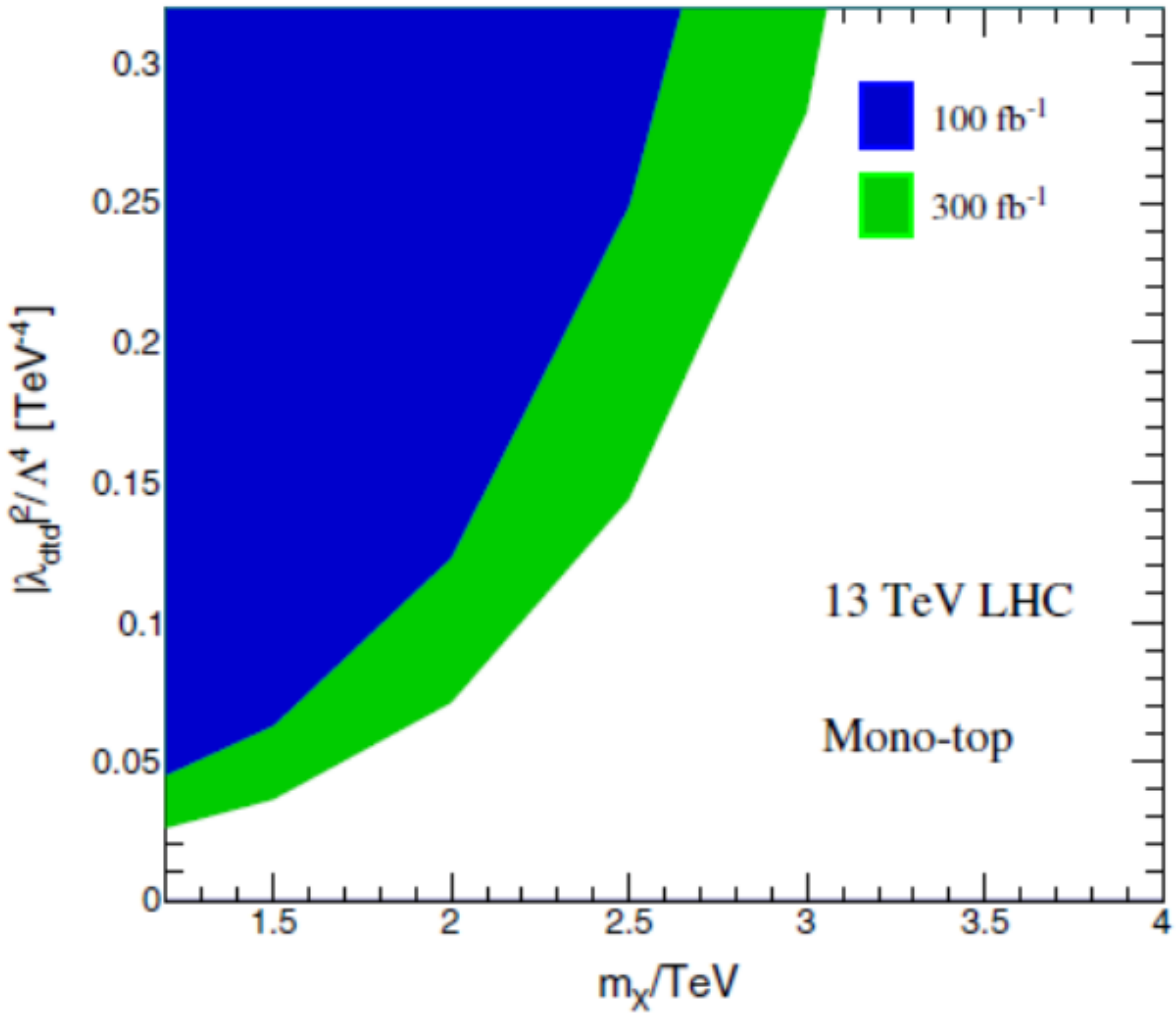

FPH, C.S. Li, **Phys.Rev. D96 (2017) no.9, 095028**

SFOPT correlates DM and GW signals.

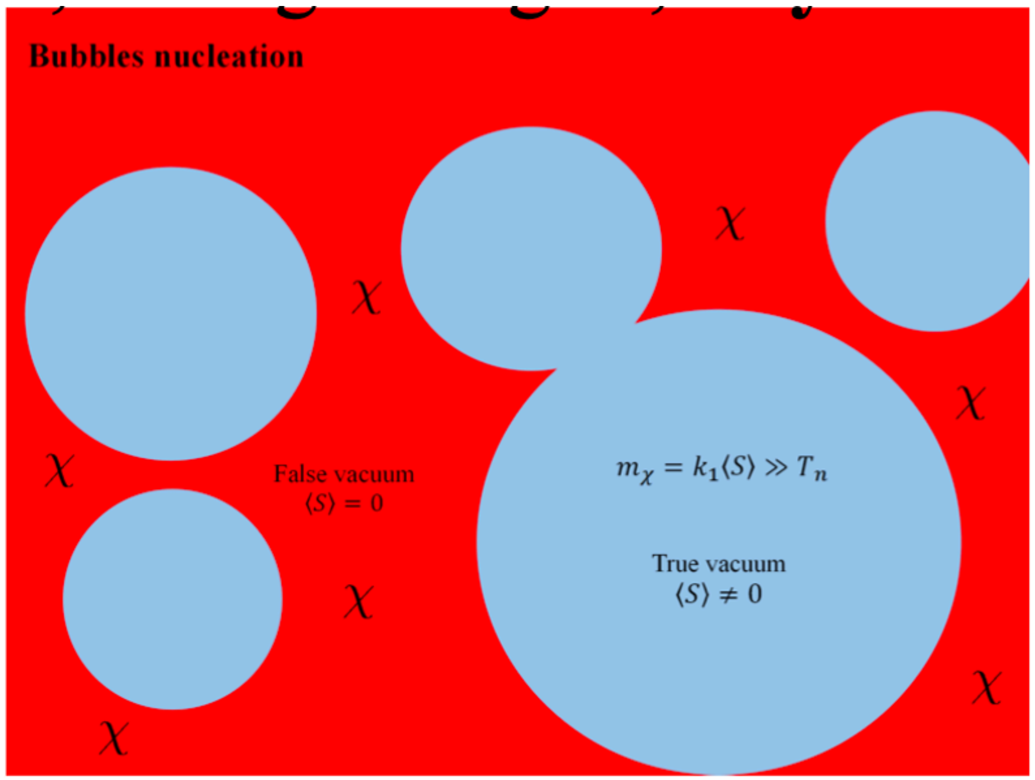

(a) Bubble nucleation:χ particles trapped in the false vacuum due to Boltzmann suppression

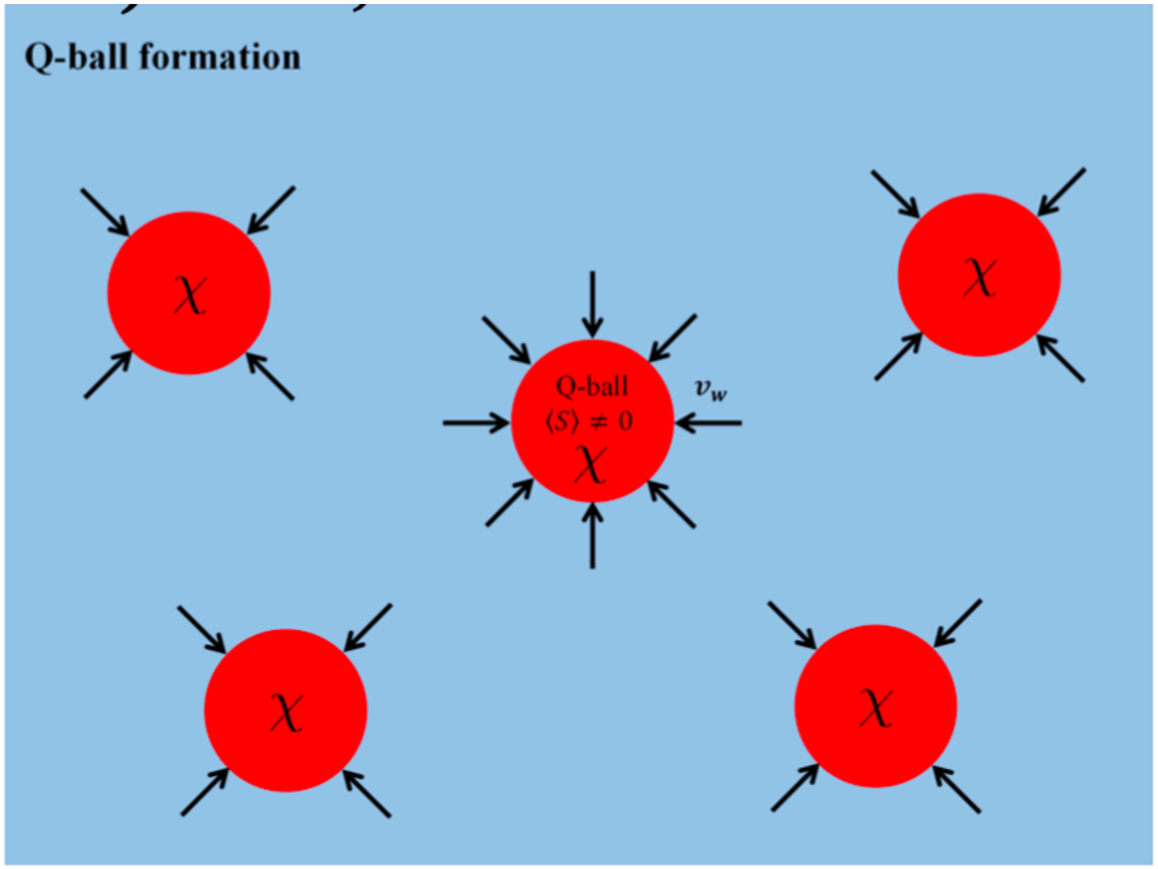

(b) Q-ball formation:After the formation of Q-balls, they should be squeezed by the true vacuum

FPH, Chong Sheng Li, Phys.Rev. D96 (2017) no.9, 095028;
FPH, Xiao Wang, this work:arXiv:2208:xxxxx

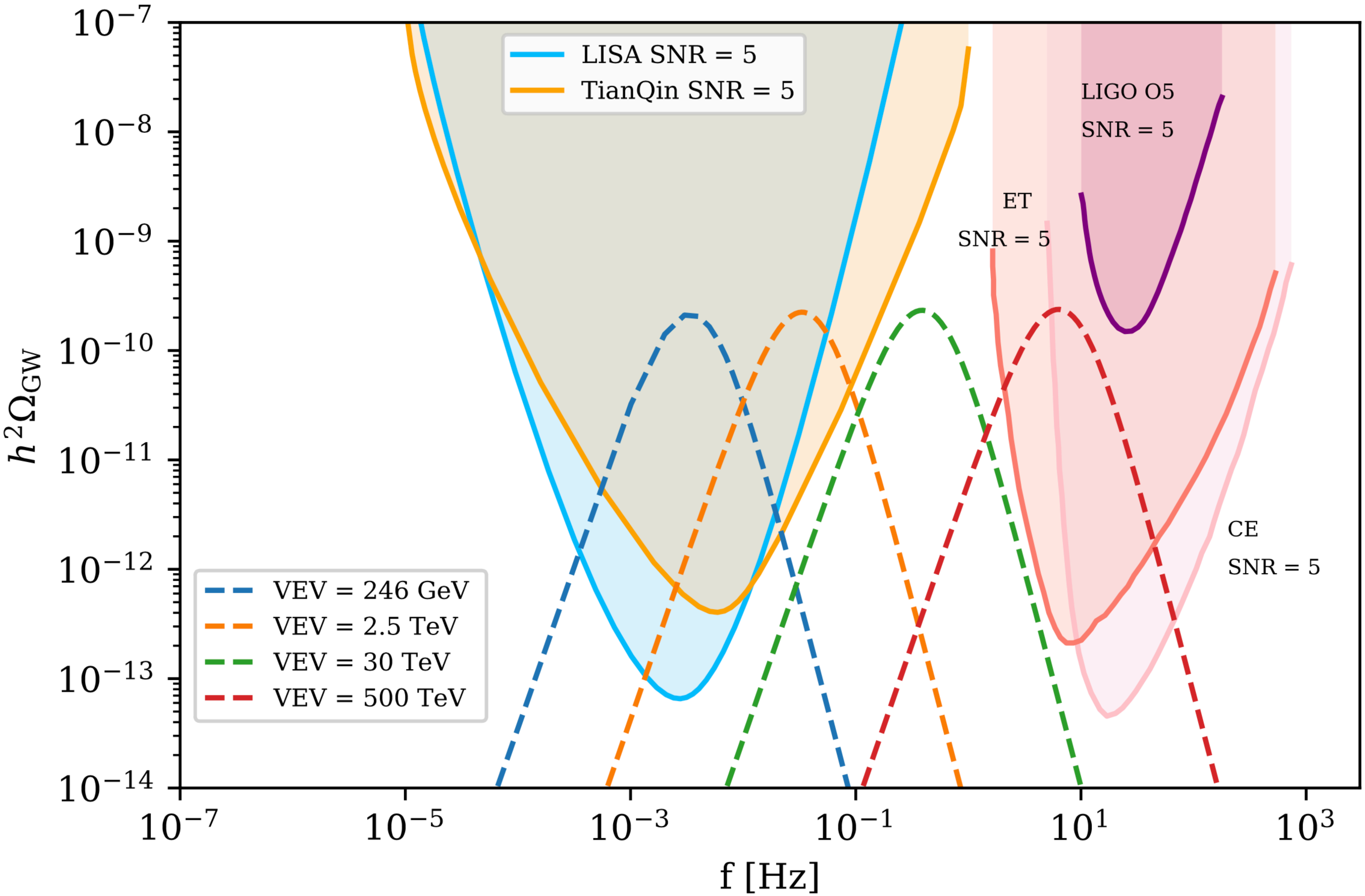

FPH, Xiao Wang, this work: arXiv:2208:xxxxx

FPH, Chong Sheng Li,
Phys.Rev. D96 (2017) no.9, 095028, cited by 38

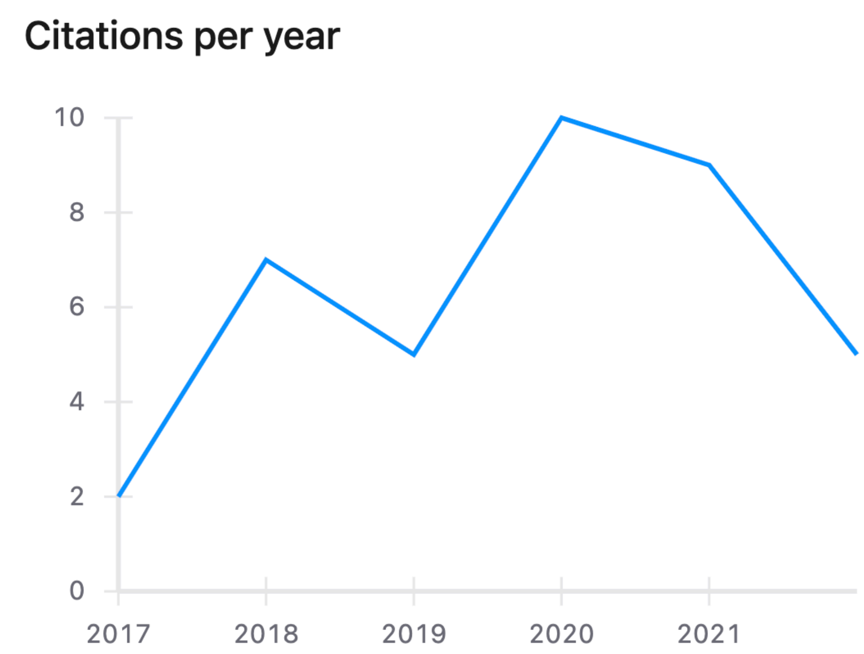

Renaissance of quark nugget DM

*B*ubbles in SFOPT can be the "filters" to packet your needed heavy DM.

FPH, Chong Sheng Li, Phys.Rev. D96 (2017) no.9, 095028
arXiv:1912.04238, Dongjin Chway, Tae Hyun Jung, Chang Sub Shin
arXiv:1912.02830, Michael J. Baker, Joachim Kopp,and Andrew J. Long
arXiv:2012.15113, Wei Chao, Xiu-Fei Li, Lei Wang
arXiv:2101.05721, Aleksandr Azatov, Miguel Vanvlasselaer, Wen Yin
arXiv:2103.09827, Pouya Asadi , Eric D. Kramer, Eric Kuflik, Gregory W. Ridgway, Tracy R. Slatyer, J. Smirnov
arXiv:2103.09822, Pouya Asadi , Eric D. Kramer, Eric Kuflik, Gregory W. Ridgway, Tracy R. Slatyer, J. Smirnov
arXiv:2008.04430 Jeong-Pyong Hong， Sunghoon Jung, Ke-pan Xie

More general cases for DM

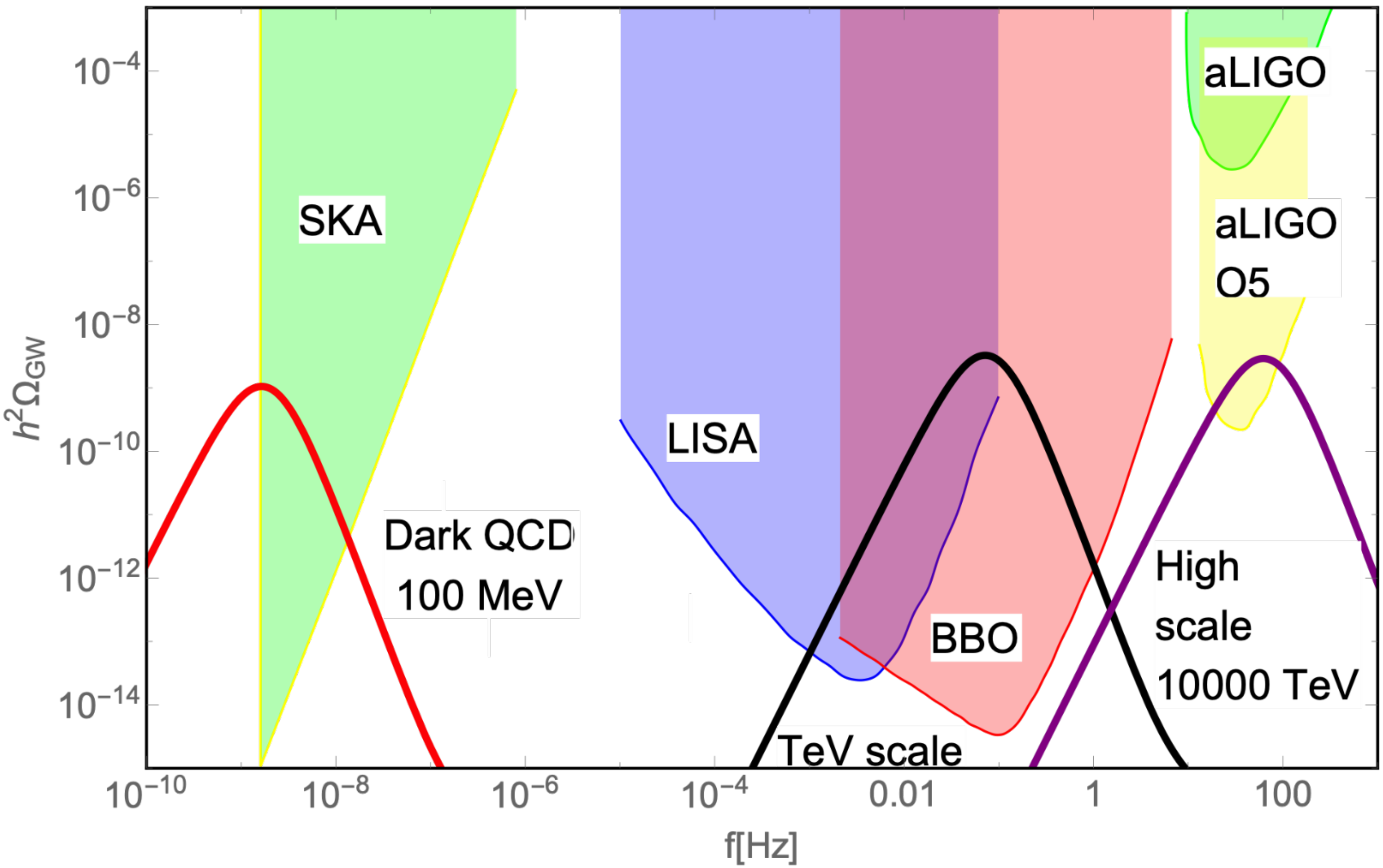

Schematic phase transition GW spectra for SKA-like and LISA-like experiments to explore DM.

FPH, Xinmin Zhang, Physics Letters B 788 (2019) 288-294

总结与展望

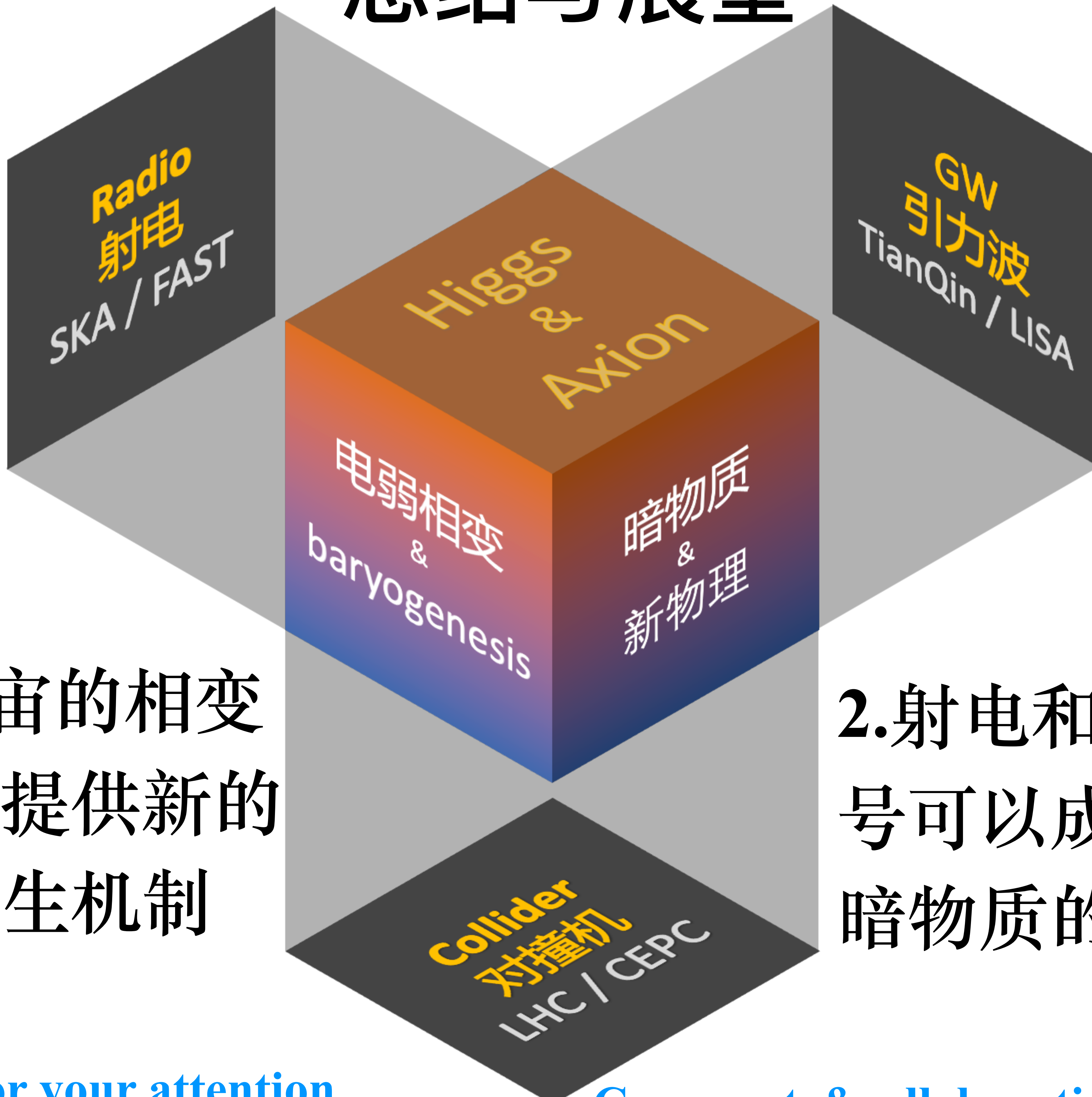

1.早期宇宙的相变过程可能提供新的暗物质产生机制

2.射电和引力波信号可以成为探测暗物质的互补方法

Thanks for your attention

Comments&collaborations are welcome

huangfp8@sysu.edu.cn